POLAR EMISSION AND EVAPORATION FROM FISSION FRAGMENTS*

BY E. PIASECKI AND J. BŁOCKI

Department IA, Institute of Nuclear Research, Świerk**

(Received May 9, 1973)

The problem of fission fragment deexcitation through the charged particle evaporation channel was investigated using the statistical angular momentum dependent model. The anticipated intensities of emission and the energy spectra of p, d, t, ^{3}He, ^{4}He, and ^{6}He, evaporated from the ^{236}U fission fragments were calculated. The results regarding α-particles explain to some extent the "polar emission" phenomenon. Assuming that the "polar" α-particles are evaporated in flight from the excited fragments the mean experimental mass of the α-emitting light fragments can be reproduced theoretically. Similarly, the α-particle energy spectrum and the intensity of emission from the heavy fragments are explained quantitatively without parameter fitting. The energy spectrum of alphas going along the light fragment trajectory can be explained if the fragment deformation is taken into account. The intensity of the last mentioned alphas and the large anisotropy of the polar alphas angular distribution can be explained only by assuming a very low value of the moment of inertia or a high angular momentum of the fragments. Suggestions are given as to carrying out further experiments as well as making use of this phenomenon in the study of fission fragment properties and in testing the statistical model of reactions.

1. Introduction

The recently performed experiment on energy-angular distribution of the α-particles emitted during the thermal neutron fission of ^{235}U gave a rather unexpected result: it was found that a measurable fraction of alphas is emitted along the fission axis [1, 2]. This phenomenon is referred to as "polar emission". It seems that the emission from the neck, characteristic of normal tripartition, is in this case hardly possible as due to the Coulomb deflection the neck-borne particles could not be registered at the fission axis. Since our first publication [1] two hypotheses concerning the nature of the polar emission have been proposed.

In Ref. [3] Halpern presumes that the mechanism of this phenomenon may be similar to that of tripartition: the separation of the nuclear matter droplet from the fragment during the violent scission process, in this case not from the neck but from the outer tip

* This work was performed under the International Atomic Energy Agency Contract No 1126/RB.

** Address: Zakład IA Fizyki Jądra Atomowego, Instytut Badań Jądrowych, Świerk, 05-400 Otwock, Poland.

of the strongly deformed fragment. The French group of Asghar *et al.* [4] interpretes the appearance of alphas at the extreme angles sa an interference effect, *viz.* a manifestation of the Fresnel-like diffraction of the usual tripartition alphas on fragments. Both hypotheses are surely attractive, but unfortunately they are not supported by calculations as yet.

In the present paper we propose another mechanism of emission of the "polar alphas", *viz.* evaporation of α-particles from the fully accelerated fragments.

As is well known, the deformation energy of the fragments is converted some time after the scission into excitation energy. Subsequent deexcitation of the fragments occurs mainly through neutron emission and partly *via* γ- and β-ray emission. The angular distribution measurements of fission neutrons proved that they are predominantly evaporated from the fully accelerated fragments, which seems to be obvious when account is taken of the estimation of the compound-nucleus reaction time [5] and of the rapidity of fragment acceleration. There are suppositions, based on two experimental works [6, 7], that a small fraction of the neutrons is emitted in the moment of scission. This is, however, unclear as there are also arguments against this guess [8, 9, 10]. Anyway, it seems obvious that other channels of fragment deexcitation (namely of evaporation of charged particles) also exist and the only question is, to what extent are these channels competitive with respect to the main one.

The fission fragments are widely distributed both as regards mass and charge. Moreover each member of the $Y(A, Z)$ distribution is characterized not only by unique parameters such as the radius, alpha and neutron binding energies, optical model parameters *etc.*, but also by certain distributions, *e. g.* of the kinetic and excitation energies $f(E_k)$ and $g(U)$, of the angular momentum $T(I)$ *etc.* The evaporation process depending on the majority of these quantities, registration of the fragments deexciting in some specific way selects from all these distributions the most "preferred" quantum numbers. The aim of the present considerations is to trace this process of selection using the available information of the fragments of the (normal) binary fission and to compare the results with the quantities measured experimentally hoping to verify in this way the hypothesis advanced.

2. Calculation of the spectra and probabilities

2.1. The method

The angular momentum dependent evaporation calculations are described in several works, to quote *e. g.* Refs [11, 12, 13].

The probability that the nucleus with excitation energy U and angular momentum I deexcites through emission of α-particles of E_α energy is given by

$$\frac{R_\alpha(U, I, U_r^\alpha)}{\sum_\nu \sum_{U_r^\nu} R_\nu(U, I, U_r^\nu)},$$

where ν are all the energetically possible ways of deexcitation. $R_\nu(U, I, U_r) = \sum_{j_r} R_\nu(U, I; U_r, j_r)$, where the $R_\nu(U, I; U_r, j_r)\, dU_r$ is the rate of emission of the particle ν of spin s with a channel

energy E_ν to form residual nuclei with spin j_r and excitation energy U_r given by

$$R_\nu(U, I; U_r, j_r)dU_r = \frac{1}{h} \times \frac{\Omega(U_r, j_r)}{\Omega(U, I)} \times \sum_{S=|j_r-s|}^{j_r+s} \sum_{l=|I-S|}^{I+S} T_l(E_\nu)dU_r.$$

Here, Ω is the spin-dependent final level density, the quantities T_l are the transmission coefficients.

$$h \sum_\nu \sum_{U_r^\nu} R(U, I; U_r^\nu) = \sum_\nu \Gamma_\nu = \Gamma_{\text{tot}}.$$

In further calculations Γ_{tot} is replaced by Γ_n whenever the excitation energy is higher than the neutron separation energy (this assumption is discussed in Section 2.4.3). Hence, in the case considered here the energy spectrum of alphas after averaging over the initial spin and excitation energy distributions $f(U, I)$ is given by

$$N(E_\alpha)dE_\alpha = \int dU \sum_I f(U, I) \times \frac{\sum_{j_r^\alpha} \Omega(U_r^\alpha, j_r^\alpha) \sum_{l=|I-j_r^\alpha|}^{I+j_r^\alpha} T_l^\alpha(E_\alpha)dE_\alpha}{\int dE_n \sum_{j_r^n} \Omega(U_r^n, j_r^n) \sum_{S=|j_r-\frac{1}{2}|}^{j_r+\frac{1}{2}} \sum_{l=|I-S|}^{I+S} T_l^n(E_n)}. \quad (1)$$

Γ_α/Γ_n ratio is given simply as

$$\int N(E_\alpha)\, dE_\alpha.$$

The probability of α-emission from the (A, Z) fragment was calculated as

$$p_\alpha(A, Z) = \frac{\Gamma_\alpha}{\Gamma_n}(A, Z) \times f_\nu(A, Z),$$

where f_ν is the probability that at least one neutron will be evaporated. As it was already stated the γ-ray competition was not considered, so the neutron evaporation was assumed to proceed in principle always whenever possible. Hence

$$f_\nu = \frac{\int_{Bn}^{\infty} g(U)dU}{\int_0^{\infty} g(U)dU},$$

where $g(U)$ is the excitation energy distribution. The cross-section $\sigma^\alpha_{L(H)}$ for producing the L or H-fragment, which deexcites through α-emission, was obtained as

$$\sigma_{\text{fiss}} \times \sum_{A=80}^{117} \sum_Z p_\alpha(A, Z) \times Y(A, Z) \quad \text{and}$$

$$\sigma_{\text{fiss}} \times \sum_{A=119}^{156} \sum_Z p_\alpha(A, Z) \times Y(A, Z), \quad \text{respectively,}$$

where $Y(A, Z)$ is the normalized yield of the (A, Z) fragments in fission.

The p_α quantity was calculated for as many as 503 nuclei produced in fission, however, the very limited core memory and speed of our GIER computer precluded direct calculation of the Γ_α/Γ_n ratio for all the relevant fragments. Instead of that we tried to factorize this ratio and to investigate the behaviour of all the factors as a function of the relevant variables. Apart from the economy in computer time this approach enabled deeper insight in the reasons of the A-variability of $\sigma^\alpha_{L(H)}$, and made easier the error analysis.

It turned out that with sufficient accuracy:

$$\frac{\Gamma_\alpha}{\Gamma_n}(A, Z) = \frac{\Gamma_\alpha}{\Gamma_n}(A_0, Z_0) \times f^{U(A)}_{B\,\mathrm{eff}\,(A,Z)} \times f^{U(A)}_{Bn\,\mathrm{eff}\,(A,Z)} \times f^{U(A)}_{Tl,Tln(A)} \times f^{U(A)}_{\Delta Z(Z)} \times f^{(U)A}_{a(A,Z)} \times f_{U(A)}. \quad (2)$$

The first factor is the Γ_α/Γ_n ratio for the "standard" nuclei, (100, 39) and (136, 53) in the case of L and H-fragments, respectively, B_{eff} is defined as $B+P(Z)+P(N)$, B being the separation energy of alphas and P the pairing energies of the residual nuclei (see Section 2.2.2), the same refers to Bn_{eff}. The fourth factor gives the dependence on the barrier penetrability when going along the fission path in the (A, Z) plane, while $f_{\Delta Z}$ is responsible for the penetrability variation when for a fixed A we depart from the most probable Z-value. The function f_a is responsible for the dependence on the level density parameter, while the last factor provides for the dependence of Γ_α/Γ_n on the excitation energy. As it is discussed further on, we assume that $g(U)$ is a Gaussian distribution, thus in Eq. (2) U actually stands for the pair of $(\bar{U}, \sigma)$ Gaussian parameters. Indexing of f-functions by U reflects the fact that the excitation energy dependence cannot be fully isolated as all factors are strongly U-dependent.

2.2. Distributions and parameters

In this Section the available data on distributions and parameters needed for calculations are discussed. A set of distributions and parameters having been selected for the main calculations, the sensitivity of the results on this choice is discussed in Section 2.4.

2.2.1. Density of levels. The Gilbert and Cameron level density formula [14] has been used:

$$\Omega(U, j) = \frac{\sqrt{\pi}}{12} \times \frac{\exp\left(2\sqrt{a(U-\Delta)}\right)}{a^{1/4}(U-\Delta)^{5/4}} \times \frac{(2j+1)\exp\left[-(j+\frac{1}{2})^2/2\sigma^2\right]}{2\sqrt{2\pi}\,\sigma^3}, \quad (3)$$

where a is the so-called level density parameter, $\sigma^2 = JT/\hbar^2$, J being the nuclear moment of inertia, T the nuclear temperature and Δ the pairing energy, $P(Z)+P(N)$. This formula was used for $U \geqslant (j+\frac{1}{2})^2/2J$ since according to the yrast level concept $\Omega = 0$ for the lower residual energy [15].

2.2.2. Separation and pairing energies. The residual energy used in Eq. (1) is defined as $U_r = U-E-B$. Separation energies of alphas, B, and of neutrons Bn, have been taken from the tables of Garvey *et al.* [16]. The pairing energies $\Delta = P(Z)+P(N)$ were taken from the work by Gilbert and Cameron [14].

2.2.3. Mass and charge distribution. Quite generally, the $Y(A, Z)$ distribution can be factorized into the $Y(A)$ and the $Y_A(Z)$ components. The first one was taken from the work

of Schmitt *et al.* [17]. As regards the $Y_A(Z)$ it is usually assumed to be a Gaussian distribution, and its parameters were determined in a significant number of works (for a review of these works see Ref. [18]). The dependence of the $\overline{Z}$ on the fragment mass is known pretty well [19], but the problem of dependence of σ_Z of this Gaussian on the mass number is unclear [20] and the available data cover a limited range of A [19, 21]. Thus we were obliged to assume that σ_Z is independent of the fragment mass. It should, however, be noted that most of the data refer to the nuclear charge distribution of the fission products rather than to that of the fragments. The value of the average (over the A) $\sigma_Z = 0.40 \pm 0.05$ (Ref. [22]) used in our calculations may be in this context compared with the post-neutron emission value of $\sigma_Z = 0.64$ given by Wahl *et al.* [18].

2.2.4. Transmission coefficients. The values of T_l for the neutrons have been taken from the tables of Marchuk *et al.* [23]. They have been calculated using the optical model, the nuclear potential of which was:

$$V(r) = \left[V_R(r) - \frac{\tau}{r} \times \frac{dV_R(r)}{dr} \times \gamma \right] (1 + i\zeta),$$

where

$$V_R(r) = \frac{-V_0}{1 + \exp\left(\dfrac{r-R}{a}\right)}; \qquad \gamma_{lj} = \begin{cases} l \text{ for } j = l + 1/2, \\ -(l+1) \text{ for } j = l - 1/2, \end{cases}$$

$$R = r_0 A^{1/3}, \quad V_0 = 45 \text{ MeV}, \quad \zeta = 0.1,$$

$$r_0 = 1.2 \text{ fm}, \quad a = 0.5 \text{ fm}, \quad \tau = 3.5 \times 10^{-27}.$$

Transmission coefficients for the alpha particles were calculated using the ALA-4 program [24] and the GIER computer. The optical model parameters have been taken from Ref. [25].

2.2.5. The cut-off parameter σ^2. This parameter is identified [5] with the mean square projection of the angular momentum $\langle M^2 \rangle$ and may depend both on excitation energy and angular momentum of the nucleus. It can be shown that $\sigma^2 = JT/\hbar^2$, where J is the moment of inertia of the nucleus. The problem of dependence of σ^2 on the excitation energy is not at all solved. In principle it is determined by the energy dependence of the J and T.

From the definition

$$T^{-1} = \frac{\partial}{\partial U} \ln \Omega(U, I = 0)$$

whence for the level density described by Eq. (3)

$$T^{-1} = \sqrt{\frac{a}{U}} - \frac{5}{4U}. \tag{4}$$

Most authors (*cf.* Ref. [11]) assume that $c = J/J_{rig} = \text{const}$, thus σ is approximately proportional to $U^{1/4}$, although there are some works ([26, 27]) in which σ was set constant.

It should be stressed that the level densities in Eq. (1) are that of the final nuclei, thus U in formula (3) and here is the residual excitation energy.

For A in the region of 80–150 and low excitation energies the value of c calculated [28, 29], determined by the isomeric ratio measurements [30] or by the angular distribution of emitted particles measurements [26] are in the range of 0.2–0.4. In terms of the superconductivity model [31], the moment of inertia should approach with increasing excitation energy the rigid body value, approximately as $J = J_{rig}(1\text{-exp}\ (-d \times U))$, with d of about 0.15, and at $U = 15$–18 MeV c should be equal to 1. The experimental facts tend to confirm this expectation. The authors of a recent work [32] prefer the relation $J = J_{rig}\ (1 - b \exp(-d \times U))$, and assuming that at $U = 0$ $J/J_{rig} = 0.3$ fit the d value as 0.10 ± 0.015 (for ^{61}Cu).

Information as to the A-dependence of c is also uncertain [33, 34]. There are guesses, at least for $A > 150$ (Ref. [35]), that the odd A nuclei have c by about 30% greater than their even-even neighbours, and the odd-odd nuclei somewhat larger than the odd-A ones. It should be emphasized, however, that the term "moment of inertia" used in spectroscopy (and in particular in Ref. [35]) has a somewhat different meaning to that given in the statistical model of reaction, where it refers to the average over the nuclear states [5]. The c values extracted from the nuclear reactions are strongly scattered [34], which may, however, be due to the experimental errors, at least in some part.

As regards spin and deformation dependence of c, it is supposed [36] that an increase of these parameters would entail the growth of the c value. However, this growth would be rather moderate, of the order of 20% when increasing I from $2\hbar$ up to $8\hbar$ [37]. Since this effect is not well established it was not accounted for in our calculations.

The main part of the calculations was performed assuming that $\sigma^2 = 1.388 \times 10^{-2}\ A^{5/3}\ cT$, which corresponds to the nuclear radius $R = 1.2\ A^{1/3}$; T being defined in Eq. (4). For c the value of 0.3 was set independently of the other variables, and in this sense it was a kind of average over them. In Sectoin 2.4 it is shown, however, that for the undeformed nuclei this assumption does not have any serious consequences.

2.2.6. Level density parameter *a*. In terms of the Fermi gas model the level density parameter $a = 2(\pi/3)^{4/3}\ \hbar^{-2} m r_0^2 A$, and equals $A/13.5$ MeV^{-1} for $r_0 = 1.2$ fm. The value of $A/8$ MeV^{-1} is, however, in better agreement with experiment, at least for nuclei far from the magic numbers [33, 38, 39], which corresponds to $r_0 = 1.57$ fm. It is supposed that this is the result of not taking account of the nuclear surface effects in the Fermi gas model on the one hand and of not taking account of angular momentum effects [11] in analysis of experimental data on the other. However, the scatter of the A/a values obtained is greater than it is usually supposed (see Refs [11, 13, 40]).

In our case the situation gets additionally complicated by the fact that the fragments have large neutron excess, while the experimental information refers mainly to the nuclei in the vicinity of the β-stability line.

An original approach for determining a of the fragments was presented by Facchini *et al.* [41]. They noticed that if the thermodynamic equilibrium is obtained at the moment

of scission, namely if $T_L = T_H$, then a simple relation occurs betweeen a_L and a_H, *viz.*

$$\sqrt{\frac{\overline{a_L}}{\overline{U_L}}} - \frac{5}{4\overline{U_L}} = \sqrt{\frac{\overline{a_H}}{\overline{U_H}}} - \frac{5}{4\overline{U_H}}.$$

Since the mean excitation energies can be more or less precisely determined from the fission neutron and γ-ray data, the quoted authors calculated $a_H(A)$ taking for $a_L(A)$ the values known for the stable nuclei. Both the assumptions mentioned are of course disputable [42].

Several semiempirical formulae exist, which try to provide for experimentally detected shell effects. The danger of such an approach lies in that here again the parameters of the respective formulae are obtained by fitting to the experimental values, known for nuclei in the vicinity of the β-stability line. As an example can serve the recently published formula [43], which gives for the $A = 100$, $Z = 39$ nucleus the improbable value of $A/a = 1.25$. The quoted author connects this breakdown of his formula with the strong deformation ($\beta \approx 0.3$) of the mentioned nucleus [44], but for the spherical nucleus $A = 143$, $Z = 53$ the result $A/a \approx 3$ does not seem reasonable either.

In the Newton formula [45] $a = 2\alpha(\bar{j}_p + \bar{j}_n + 1)\, A^{2/3}$ MeV^{-1} averages are used of spins over the single particle states adjacent to the Fermi level; they were taken from the old work of Klinkenberg [46]. In a somewhat more recent work [47] the values of $\bar{j}$ were calculated account being taken of the pairing effects. The numerical constant 2α was determined as 7.48×10^{-2} (Ref. [48]) or $(9.5 \pm 0.7) \times 10^{-2}$ (Ref. [47]). Lang [50] tried to extract the information on the $a(A)$ dependence for fragments from analysis of the fission neutron data, and obtained in the region of heavy fragments values smaller than those given by formula from Ref. [48] by a factor of about two. Unfortunately, he was unable to conclude which results are recommended.

In the probably most recent attempt of going along this line [49] the authors assumed that the coefficient 2α is a function of A and N–Z, and by fitting three parameters they were able to describe all a values known from experimental neutron spectroscopy.

The semiempirical formula of Gilbert and Cameron [14] gives very pronounced shell effects, but the authors stressed that their formula holds definitely worse in the close neighbourhood of the magic numbers.

The problem of energy dependence of the level density parameter seems to be even further from solving. Bodansky [51] presumes that the shell effects would decrease with increasing U, but he does not give any numerical estimates. The author of Ref. [52] bases on the Newton-Lang approach and takes account of the fact that the averaging of j values is dependent on the number of excited states. Going along this line we estimated that in our case a change of U from 10 to 5 MeV may be responsible for a 15% change of the a value. This effect seems, however, to be too uncertain to be included in our calculations.

A comparison of A/a values in the interesting region of A is shown in Fig. 1.

Taking into account the scatter of results we decided to perform calculations assuming two sets of $a(A)$ values: (*i*) putting $A/a = 7$ for the L and $A/a = 9$ for the H fragments, respectively, and (*ii*) for comparison using the Gilbert-Cameron values (Ref. [14]).

2.2.7. The $f(U, I)$ distribution. The information on this function being very limited, it was assumed that it can be factorized into the two independent distributions $g(U)$ and $T(I)$.

2.2.7a. The excitation energy distribution $g(U)$. When the fragments are fully accelerated the potential (excitation + deformation) energy is the difference between the fixed, for the particular mass and charge ratio, Q of reaction and the Gaussian-like distributed kinetic energy. It is usually assumed [36, 53–56] that the excitation energy of the frag-

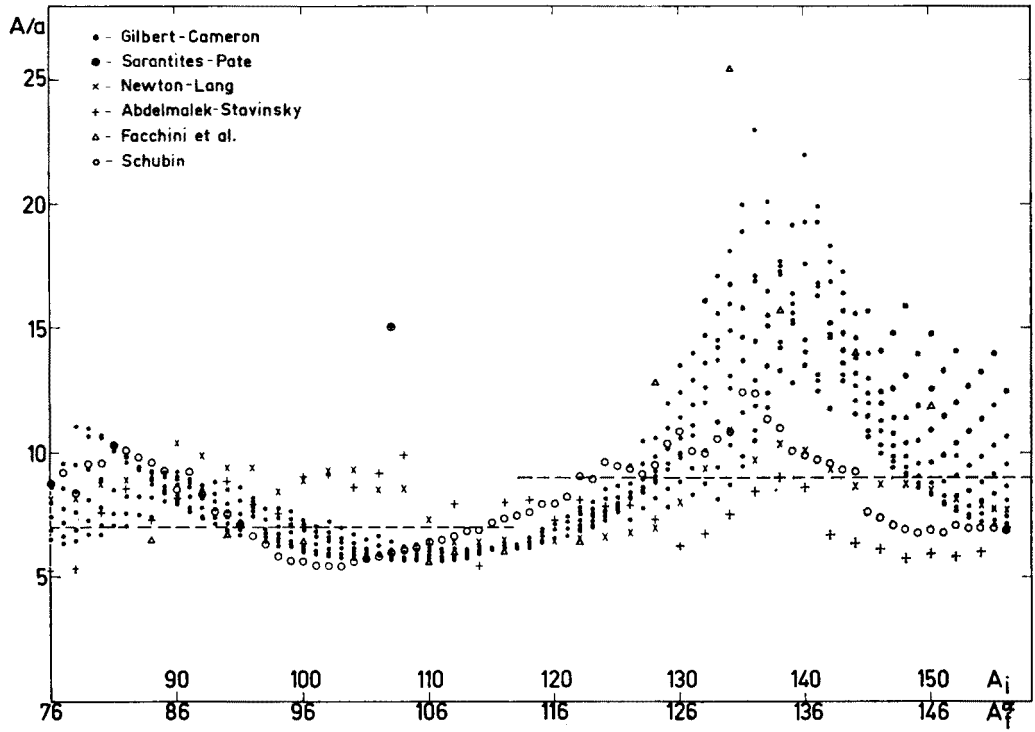

Fig. 1. Comparison of the A/a values resulting from various semiempirical formulae [14, 41, 47, 48, 49] The points obtained from the Gilbert-Cameron formula [14] illustrate also the dependence on Z. For other cases only the values for nuclei from the "fission path" are shown. The result of experimental work of Sarantites and Pate [13] concerns the $^{107}Ag+\alpha$ reaction

ments of particular (A, Z) values also shows a Gaussian distribution. Most frequently the mean excitation energy of the fragments is estimated from the fission neutron and γ-ray data. The main difficulties are connected, however, with the estimation of the $g(U)$ width.

It is usually assumed that $\sigma^2_{E_{\text{kin}}} = \sigma^2_{U_{\text{pair}}}$, where U_{pair} is the excitation energy of both the fragments, what is equivalent to assumption that the deformation energy is not smeared. Moreover, there is one more source of smearing of the excitation energy of individual fragments. Although it seems probable that almost all the excitation energy is due

to the fragment deformation energy at scission and that the internal excitation shared between the fragments in the scission moment is low [42], there are experimental guesses [57, 58] that there exist some fluctuations in the sharing of U_{pair} between the fragments, even for fixed mass and charge ratios and kinetic energies. This may be for instance due to that the deformation of the particular fragment has its own distribution [59]. Details of this sharing are not known, and it is difficult therefore to pass from $\sigma^2_{U_{\text{pair}}}$ to the variance of $g(U)$ referring to the individual fragments. Some authors simply assume the relevant

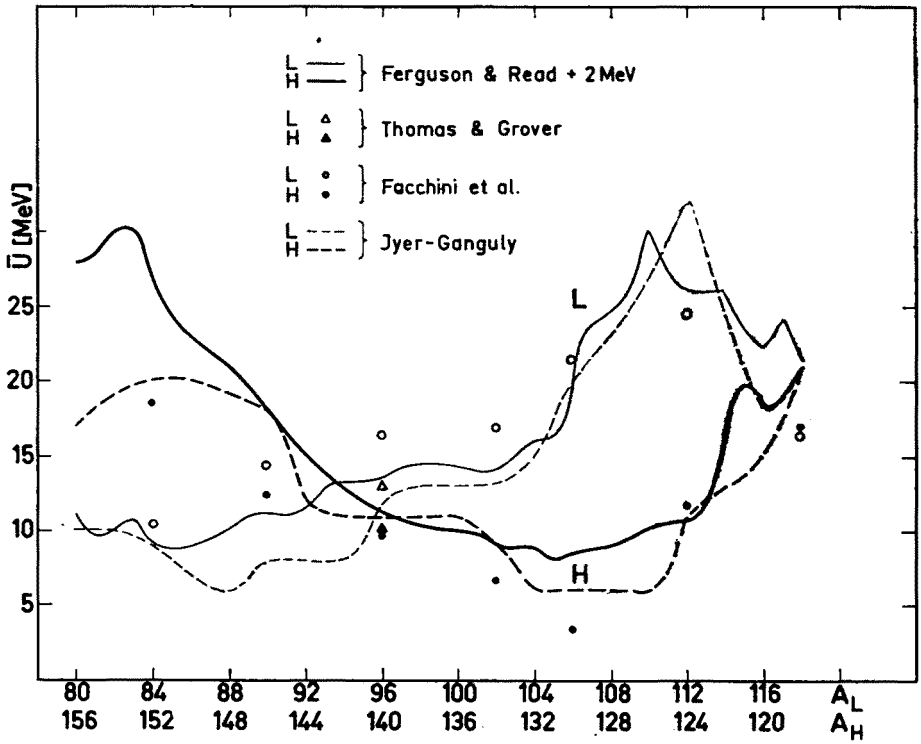

Fig. 2. Compilation of data [41, 54, 60, 63] concerning the dependence of the mean excitation energy of the fragments on their mass number. The results of Iyer and Ganguly [63] are purely theoretical

values, *e. g.* $\sigma = 2.1$ MeV [56] or 3.4 MeV [55], independently of the mass and charge of the fragments. Other assumptions concern the correlation coefficient ϱ between the $g(U)$ distributions of the light and heavy fragments in the pair, *viz.*

$$\sigma^2_{U\text{pair}} = \sigma^2_L + \sigma^2_H + 2\varrho\sigma_L\sigma_H. \tag{5}$$

In Ref. [60] ϱ is assumed to be $+1$, in Refs [53] and [54] $\varrho = 0$, both choices are made without any justification. According to Ref. [58] ϱ "is substantially lower than $+1$ at least for some portion of the fragment mass-ratio distribution". The two recent works, of Nifenecker [61] and of Signarbieoux [62] being done due to the same method, gave opposite results: while Nifenecker came to the conclusion that a strong anticorrelation

exists between the excitation energies of both fragments, the authors of second work state that this correlation "does not exist apart from a small region around $A = 99$". Theoretical predictions are rather uncertain. Nix and Swiatecki [36] depending on the assumed temperature and viscosity of fragments obtained in terms of the liquid drop model values between -0.44 and -0.58, referring to the fission of $^{213}_{85}$At.

Moreover, to obtain from Eq. (5) the values of σ_L and σ_H the value of the σ_L/σ_H ratio should be assumed. Most authors assume [53, 54, 60] that $\sigma_L^2/\sigma_H^2 = \overline{U}_L/\overline{U}_H$. In our calculations we have based on the work of Ferguson and Read [54]. The latter authors used

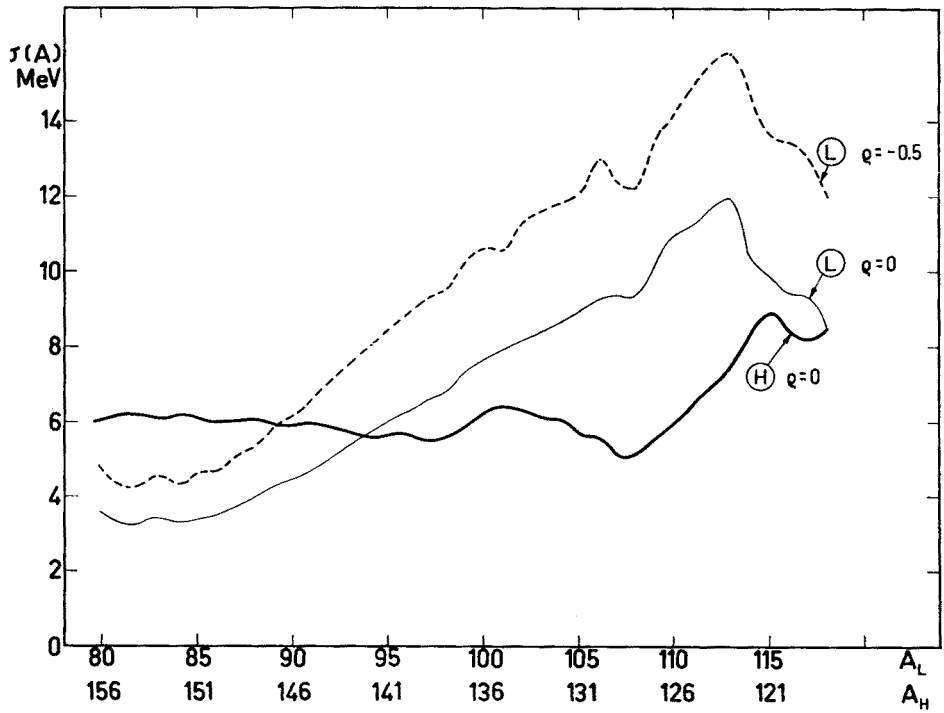

Fig. 3. Dependence of the Gaussian parameter σ of the excitation energy distribution $g(U)$ on the mass number A

a somewhat oversimplified approach to the problem of neutron evaporation from the fragments, and fitted the $\overline{U}(A)$ values in order to reproduce the experimental data regarding $\nu(A)$. It is easy to indicate the shortcomings of the method used: it did not take account of the yrast level and γ-ray competition effects, the excitation energy was assumed to be independent of Z (for a particular A), the cut-off of $g(U)$ at $U = 0$ was apparently disregarded, the data regarding $\nu(A)$ are not very well established, the distribution of neutron energy was approximated using the mean value, and the assumptions as to the ϱ and σ_L/σ_H ratios were not given adequate justification. It is not surprising therefore that the distribution of neutron emission multiplicity obtained differs distinctly from the experi-

mental one. The work has, however, at least one great advantage: it is the only one, known to us, which gives the relevant values obtained in a consistent way for the whole area of A of interest.

As it was said we used the $\bar{U}(A)$ values from Ref. [54], but tried to provide in some extent for the γ-deexcitation channel by increasing, according to the hint in [54], the $\bar{U}$ values by 2 MeV. From these $\bar{U}$ values we recalculated the $\sigma(A)$ dependence assuming that $\varrho = 0$ and $\sigma_L^2/\sigma_H^2 = \bar{U}_L/\bar{U}_H$, $\sigma_{\text{kin}}^2(A)$ was taken from Ref. [17]. A comparison of the $U(A)$ values used with other data available and $\sigma(A)$ are shown in Figs 2 and 3, respectively.

2.2.7b. Angular momenta. All the available experimental information on the angular momenta of fragments was obtained by measuring the characteristics of fission γ-rays. In this way the results refer to the fragments after the neutron and γ-ray deexcitation, and any conclusions as to the spins of the primary fragments are burdened with many assumptions.

Strutinsky [64] explained the γ-ray anisotropy assuming $\bar{I}$ of the order of 20 $\hbar$, preferentially perpendicularly oriented with respect to the fission axis. Much lower values were obtained [65] from the isomeric ratio measurements: for ^{81}Se and ^{83}Se the $\bar{I}$ value was 7 $\hbar$, for ^{131}Te and ^{133}Te $\bar{I} = (5 \pm 1.5)\ \hbar$ (Ref. [66]). The above results refer to low-energy fission of ^{239}Pu and ^{235}U, respectively. By measurement of the isomeric ratio of ^{134}Ce from photofission of ^{233}U the value of 6.5 $\hbar$ was obtained [67]. Very instructive is the case of two works (Refs [68] and [69]) published simultaneously: both authors obtained the same anisotropy of γ-rays, of 10–15 per cent, however, their analysis resulted in quite different angular momenta of the fragments. While Hoffman [69] gives $I = (7 \pm 2)\ \hbar$, when referring to the time after the neutron emission, the authors of Ref. [68] obtained $\bar{I} = 11\ \hbar$ after the γ-cascade and speculated that at the beginning of the γ-deexcitation the mean spin is yet a few units greater and before the neutron evaporation it is of the order of 20 $\hbar$.

Somewhat similar ambiguities are characteristic of the work [70] in which the γ-anisotropy in the thermal neutron fission of ^{235}U was measured. Owing to the poor knowledge of the γ-deexcitation mechanism, the results of experiment were difficult to interprete, and depending on the model used $\bar{I} \leqslant (16 \pm 2)\ \hbar$ or equal to $(8 \pm 2)\ \hbar$. Unfortunately, none of these models give the proper dependence of anisotropy on the fragment mass (experimentally found to be very weak). Also a weak dependence on A for spontaneous fission of ^{252}Cf was found in a recent work of Wilhelmy *et al.* [71]. The authors assumed that the angular momentum distribution is of the shape of $T(I) \sim (2I+1) \exp\ [-B^{-2}I(I+1)]$, and interpreted the intensity of gammas assuming $\bar{I} = (6.5 \pm 1)\ \hbar$, and from the anisotropy of the gammas determined $\bar{I} = (5.5 \pm 1)\ \hbar$.

The scanty theoretical results are not less ambiguous. Hoffman [69] calculated that $\bar{I}$ should be of the order of 5–6 $\hbar$. According to Ref. [36], dealing with the fission of $^{213}_{85}$At, at the moment of scission the average value of I is of about 10 $\hbar$, and due to electromagnetic interaction between the fragments their angular momenta increase to 12–18 $\hbar$, depending on the viscosity assumed. The work of Rasmussen *et al.* [72], in which angular oscillations are calculated occurring when the fragments pass from the scission to the equilibrium

deformation, gives the value of $\bar{I}_{sciss} = 5.6\ \hbar$. This value due to electromagnetic interaction increases up to 6–8 $\hbar$ (this result refers to the ^{108}Ru fragment from the thermal neutron fission of ^{239}Pu).

It should by noted that important is not only the value of $\bar{I}$ but also the shape of $T(I)$ distribution, since for low values of c the high-spin tail of $T(I)$ plays a predominant role.

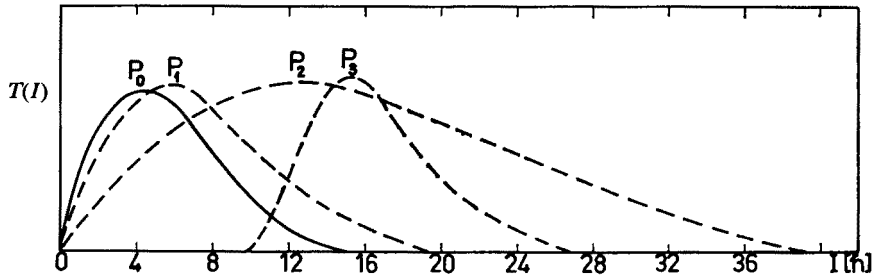

Fig. 4. Distributions of the initial angular momentum of fragments. The curve P_0 was calculated by Rasmussen *et al.* [72] without taking account of the Coulomb effects, including of which should give the P1 distribution. Distributions P2 and P3 have the mean values of spin twice as large as P1. They were used for testing of our results sensitivity to the assumed spin distribution

Basing on the shape of $T(I)$ calculated in Ref. [72] we supposed that the $T(I)$ is given by the P1 distribution of Fig. 4. We assumed that this distribution is independent of all other variables, but we examined the eventual consequences of this assumption performing also the calculations making use of the P2 and P3 distributions.

2.3. Results

The dependence of the Γ_α/Γ_n ratio on the relevant variables is shown in Figs 5–9. The values of the f-functions (defined in Eq. (2)) for all the 503 nuclei of interest were read off the curves of this kind. The p_α and σ_α values for some nuclei are shown in Table I. The result of averaging over the nuclear charge is shown as $p_\alpha(A)$ in Fig. 10. The effect of multiplying it by the mass-yield or the cross-section dependence on the mass number for the two variants of the $a(A)$ dependence may also be seen from this figure.

An approximate estimate of the importance of various factors can be inferred from Fig. 11, where the averages of the f-functions over Z are shown. (This approximation is due to the fact that when calculating the cross-section we deal with Z-averaging of the product of f-functions, which differs somewhat from the product of averages.)

Fig. 5. Function $f_{B\text{eff}}$ or dependence of the Γ_α/Γ_n ratio on α-particle separation energy, defined as

$$\frac{\frac{\Gamma_\alpha}{\Gamma_n}(B_{\text{eff}},\ \bar{U},\ \sigma,\ \text{other parameters}\ (A_0, Z_0))}{\frac{\Gamma_\alpha}{\Gamma_n}(B_{\text{eff}}\ (A_0, Z_0),\ \bar{U},\ \sigma,\ \text{other parameters}\ (A_0, Z_0))}.$$

This figure refers to the heavy fragments, thus $A_0 = 136$, $Z_0 = 53$. For light fragments the curves are very similar, but because $A_0 = 100$ and $Z_0 = 39$ the intersection point is at $B = 7.9$ MeV. Numbers in parentheses are the $\bar{U}$ and σ parameters of the Gaussian distribution of excitation energy $g(U)$

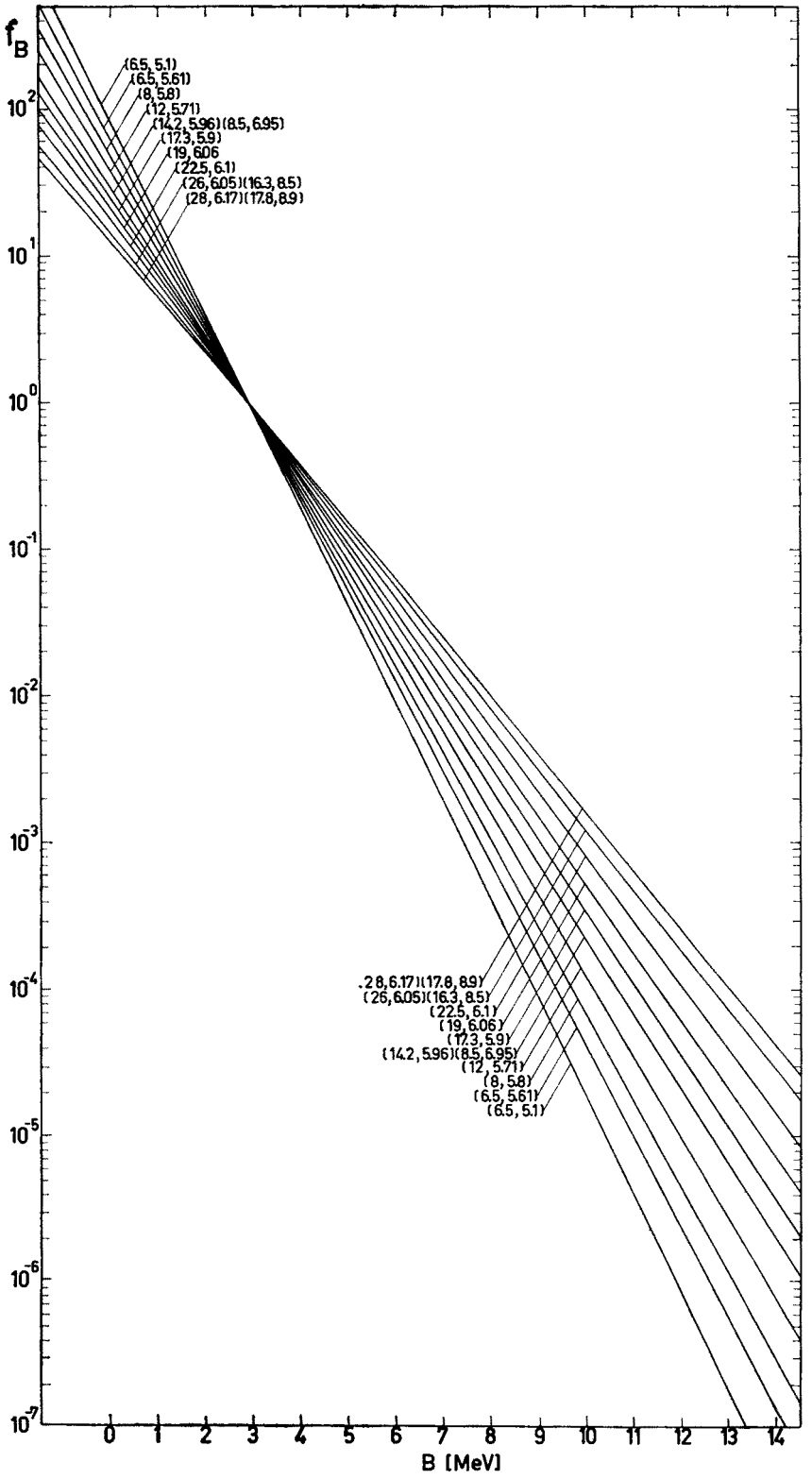
f_B
10^{2}
10^{1}
10^{0}
10^{-1}
10^{-2}
10^{-3}
10^{-4}
10^{-5}
10^{-6}
10^{-7}
(6.5, 5.1)
(6.5, 5.61)
(8, 5.8)
(12, 5.71)
(14.2, 5.96)(8.5, 6.95)
(17.3, 5.9)
(19, 6.06
(22.5, 6.1)
(26, 6.05)(16.3, 8.5)
(28, 6.17)(17.8, 8.9)
(28, 6.17)(17.8, 8.9)
(26, 6.05)(16.3, 8.5)
(22.5, 6.1)
(19, 6.06)
(17.3, 5.9)
(14.2, 5.96)(8.5, 6.95)
(12, 5.71)
(8, 5.8)
(6.5, 5.61)
(6.5, 5.1)
0
1
2
3
4
5
6
7
8
9
10
11
12
13
14
B [MeV]

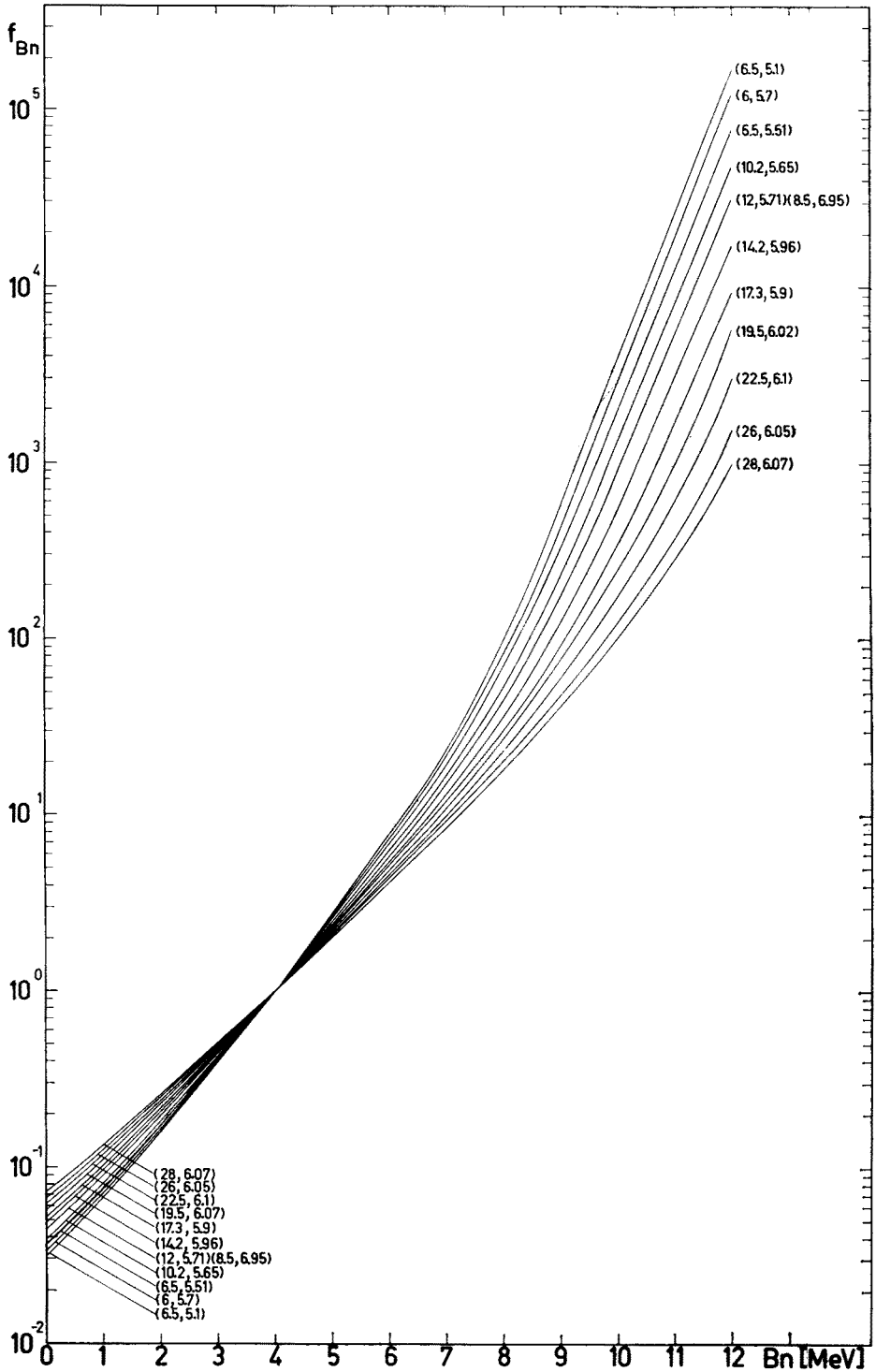

Fig. 6. Function $f_{Bn\,\mathrm{eff}}$ or dependence of the Γ_α/Γ_n ratio on the neutron separation energy. This function is defined analogously as $f_{B\mathrm{eff}}$

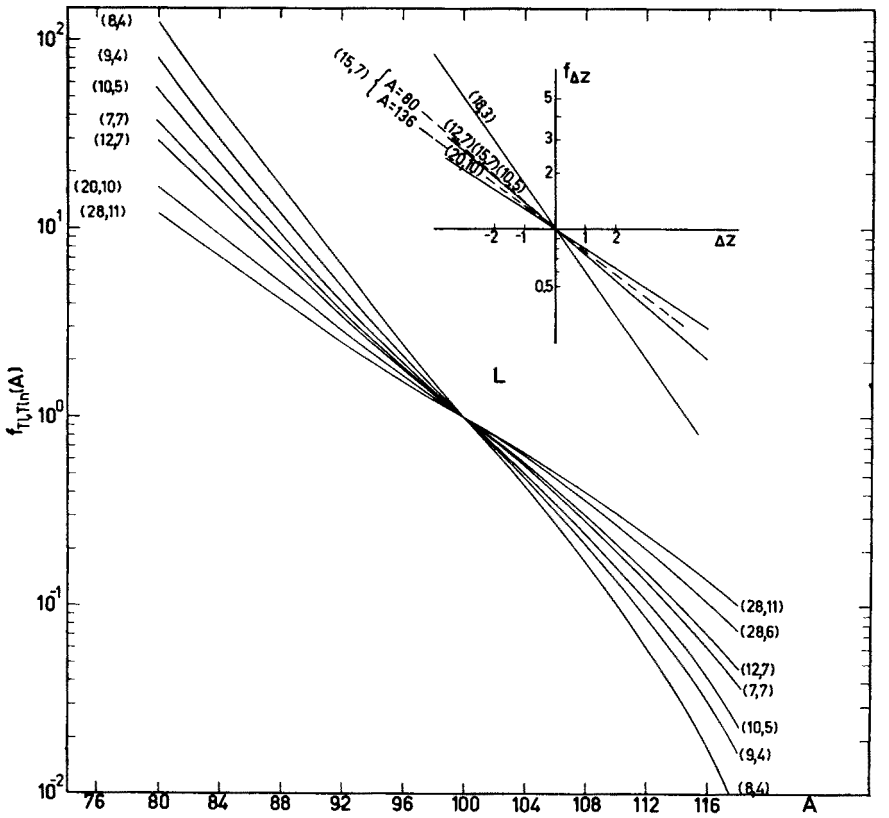

Fig. 7. Function $f_{Tl,Tln}$ giving the variation of the Γ_α/Γ_n ratio with barrier penetrability changing with the mass number. It is defined as

$$\frac{\dfrac{\Gamma_\alpha}{\Gamma_n}(A, \overline{U}, \sigma, \text{optical model parameters } (A), \text{ other parameters } (A_0, Z_0))}{\dfrac{\Gamma_\alpha}{\Gamma_n}(A_0, \overline{U}, \sigma, \text{all other parameters of } (A_0, Z_0))}$$

and was calculated for the nuclei from the "fission path". Function $f_{\Delta z}$ gives the change of penetrability when we are departing from the "fission path" and is defined similarly. Note the moderate dependence on the mass number

The integral cross-section and the mean masses of the fragments evaporating an α-particle were obtained from the $\sigma_\alpha(A)$ (Table II). The experimental and calculated (for the mean masses) E_α^{peak} of alpha spectra in the lab-system are also compared in that Table.

The calculated spectra of α-particles evaporated from some typical fragments are presented in Fig. 12. If the calculated spectra are transformed to the lab-system then it appears that the differences between the evaporation spectra for different fragments are greatly compensated due to the differences in masses and velocities of these fragments. Moreover, the kinetic energy distribution of fragments having a fixed A-value entails smearing the α-particle spectra both in c. m. s. and the lab-system by less than 4 per cent. The result is the apparently strange [3] narrowness of the polar emission spectra.

2.4. Is it possible to improve the results?

The situation may be recapitulated as follows: the agreement of calculations with experiment seems to be reasonable considering the spectrum and yield of alpha particles evaporated from the heavy fragments. The mean mass of the L-fragments in the polar emission process may also be explained (the experimental value of $\bar{A}_H$ is unknown). The

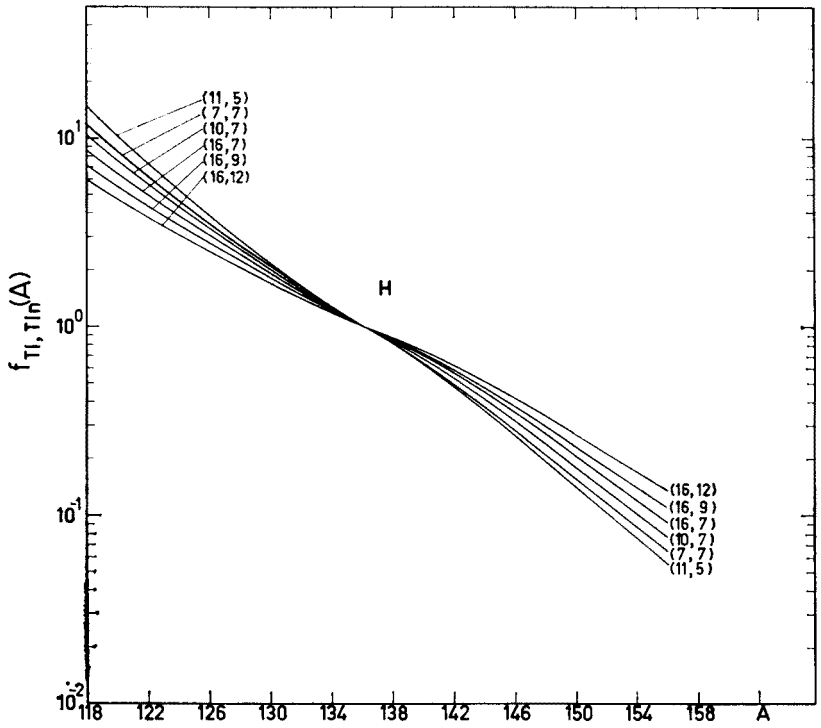

Fig. 8. Function $f_{Tl,Tln}$ for heavy fragments

spectrum of alpha particles emitted from the light fragments is similar to the calculated one, however, the latter is by about 2 MeV too high (in the lab-system) and the experimental yield is definitely (about 12 times) greater than that calculated. However, from these disagreements nothing may be concluded before the possible consequences of the approximations done and the uncertainties of parameters used are discussed.

2.4.1. Separability. Of course, if dependence on one variable would substantially depend on others, the discussion of errors would be very cumbersome. Fortunately, during the calculations we found that *e. g.* the dependence of Γ_α/Γ_n on the binding energy B is independent of Bn and *vice versa*, and that the dependence on the nucleus and on the value of the moment of inertia c is weak. The dependence on Z changes but slightly with A; similarly the dependence on the excitation energy only slightly changes with c, nucleus and angular momentum distribution. Quantitatively speaking, we calculated the Γ_α/Γ_n

strictly and compared the results with the approximate outcome of Eq. (2) for 20 nuclei of various (A, Z), and the disagreement was usually within the limits of 10–15 per cent. There was one case in which the disagreement reached the factor of 10, however, this occurred for a nucleus with parameters extremely different from the average ones. Taking

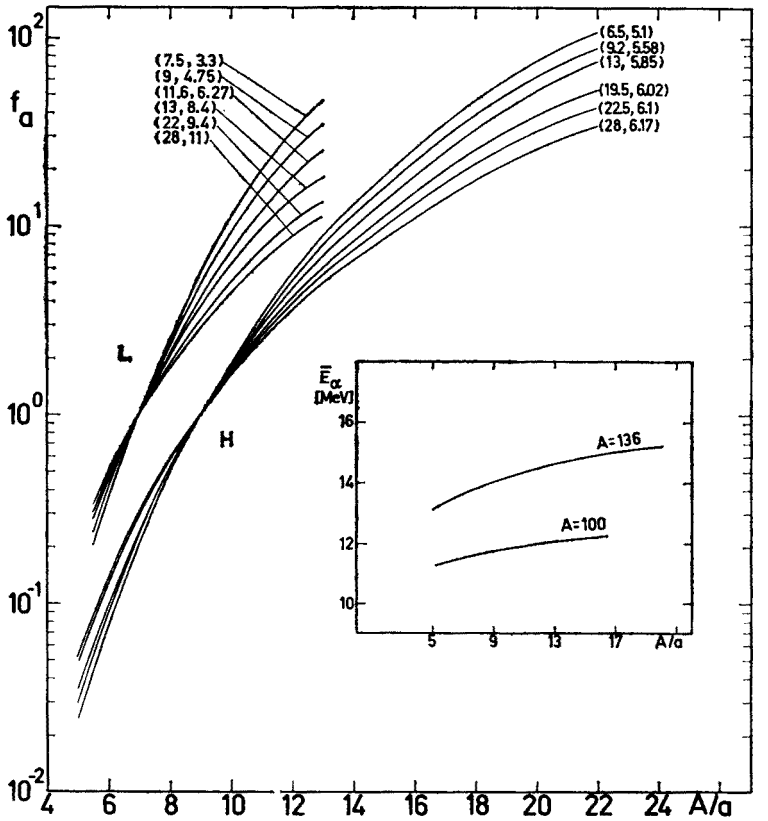

Fig. 9. Dependence of the Γ_α/Γ_n ratio on the A/a value for L- and H-fragments. The dependence of the mean energy of alphas (in the fragment reference system) on A/a is given too. Note that with increasing of α-emission intensity, $\bar{E}_\alpha$ rises as well

into account that Eq. (2) holds worse for nuclei giving only small contribution to the total cross-section, we estimate the maximum error of σ_α due to the separability assumption at about 10 per cent.

2.4.2. Yrast levels. The angular momentum has, generally speaking, a great effect on the Γ_α/Γ_n ratio (see Fig. 13). However, when the spin distribution is given by P1 (Fig. 4), this effect is not of primary importance. The well known Weisskopf-Ewing formula [73] gives in our case results approximately correct. This formula formally can be obtained from Eqs (1) and (3) when it is assumed that σ is independent of the excitation energy and the c value tends to infinity. The result is shown in Fig. 14.

TABLE I

Probability of α-particle evaporation p_α and the cross-section σ_α for production of the α-deexciting fragment in a thermal neutron fission of ^{235}U as a function of A and Z of the fragments

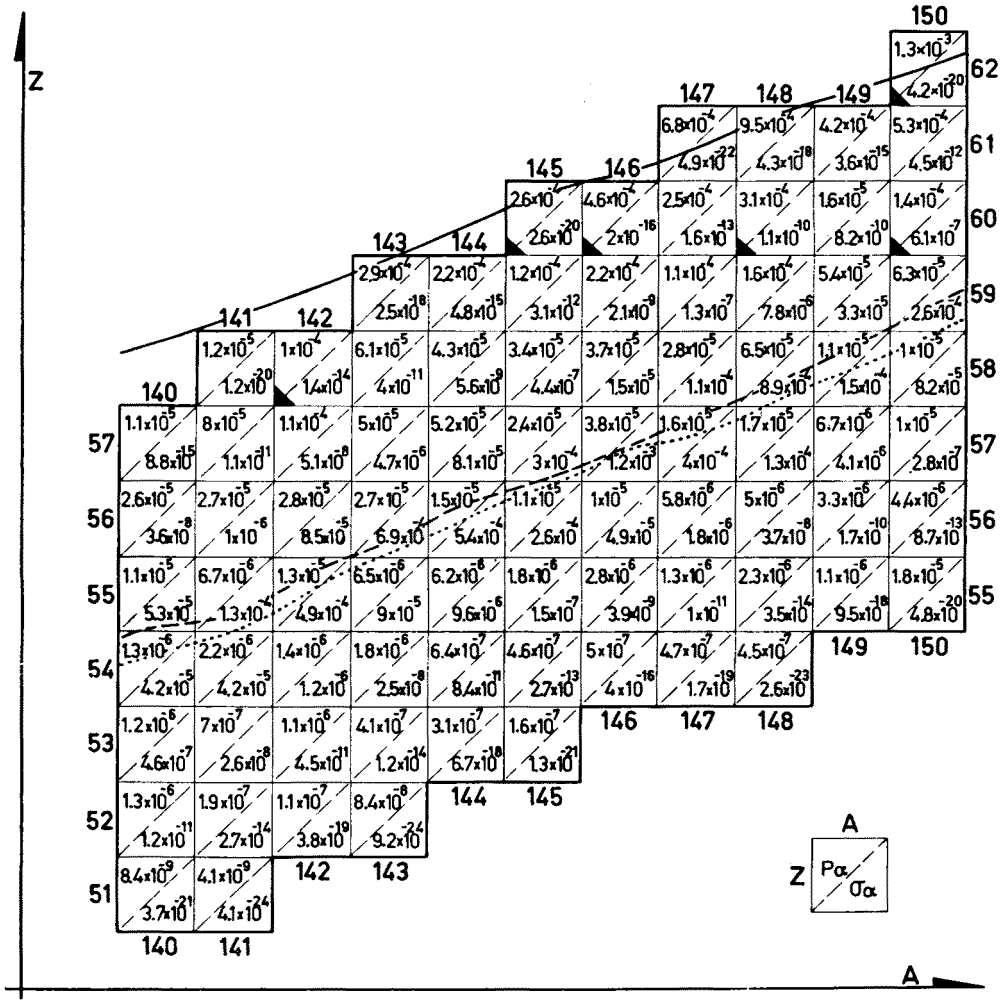

The β-stability line and the fission path are given by the solid and dotted line, respectively. The dashed curve joining the most probable α-emitting fragments practically overlaps the dotted one. Stable nuclei are marked with black triangles.

Somewhat similar is the situation for yrast levels (YL). Comparing different methods of calculating YL Thomas has shown [34] that for $I < 15\ \hbar$ they give similar results, thus we used the simplest formula $[\hbar^2 I(I+1)]/2J$. For distribution of angular momenta given by P1 the inclusion of YL into calculations practically influenced neither Γ_α/Γ_n nor $\bar{E}_\alpha$, for P2 and P3 distributions, however, the effects of YL were distinct.

The method of including YL into the calculations, followed after Sperber and Thomas

[15, 11], suffers from the sharp cut-off effects. Probably more correct is the approach of Sarantites and Pate [13] according to which YL's are included into the level density formula as follows:

$$\varrho(U, I) = \frac{\sqrt{2}}{48}\left(\frac{\hbar}{J}\right)^{1/2} a^{1/2}(U'+t-E_{\mathrm{rot}})^{-2}(2I+1)\exp\{2[a(U'-E_{\mathrm{rot}})]^{1/2}\},$$

$$U' \equiv U-\Delta, \quad E_{\mathrm{rot}} \equiv \frac{\hbar^2 I(I+1)}{2J}. \tag{6}$$

t is calculated from the relation $U' = at^2 - t$. In the case of P1 spin distribution this method gives values of the Γ_α/Γ_n ratio by 50 per cent greater than our standard approach, when $c = 0.3$, but for larger moments of inertia this difference decreases rapidly. When $T(I)$ is given by the P2 or P3 distribution, the difference for $c = 0.3$ is larger by many orders of

TABLE II

Comparison of the experimental and calculated cross-sections and energies of α-particles

		σ_α, mb		$\overline{A}^p$		E_α^{peak}, MeV	
		L	*H*	*L*	*H*	*L*	*H*
Experimental		21±4	6±2	98.4±1.3	?	23.5±1[c]	22.7±1.5
calculated	a	1.7	7.0	100.7	146.1	25.7	24.0
	b	1.1	37.7	99.3	142.7		

[a] $A/a = 7$ for the *L*-and 9 for the *H*- fragments were assumed (*i.e.* $f(a) = 1$).
[b] A/a as a function of (A, Z) taken from the Gilbert-Cameron tables [14].
[c] Estimated maximum uncertainty, the main part of which is due to the systematic calibration error.

magnitude (see Figs 13 and 14), but these cases may probably be excluded from the considerations as the alpha spectrum is then unreasonably high. For P1 initial spin distribution the spectra calculated accordingly to both methods differs by about 0.1 MeV. Thus it may be concluded that our σ_α values are probably too low, but the error seemingly did not exceed 50 per cent.

2.4.3. The γ-ray competition. We neglected the γ-ray competition assuming that

$$\Gamma_n/\Gamma_{\mathrm{tot}} = \int_{Bn}^{\infty} g(U)dU \Big/ \int_0^{\infty} g(U)dU.$$

Actually, as is known from the works of Grover and Gilat [12] when the excitation energy is lower than approximately $Bn+\mathrm{YL}$, the γ-deexcitation predominates. It was shown in Ref. [60] that when this effect is accounted for the calculated $\bar{\nu}$ value decreases by about 15 per cent.

There were two reasons for making our assumption: the gamma transition strengths are quite uncertain, and besides the parameters of the $g(U)$ distribution were fitted by Ferguson and Read [54], neglecting the γ-ray effect so it would not be consistent to account for these effects *ad hoc*.

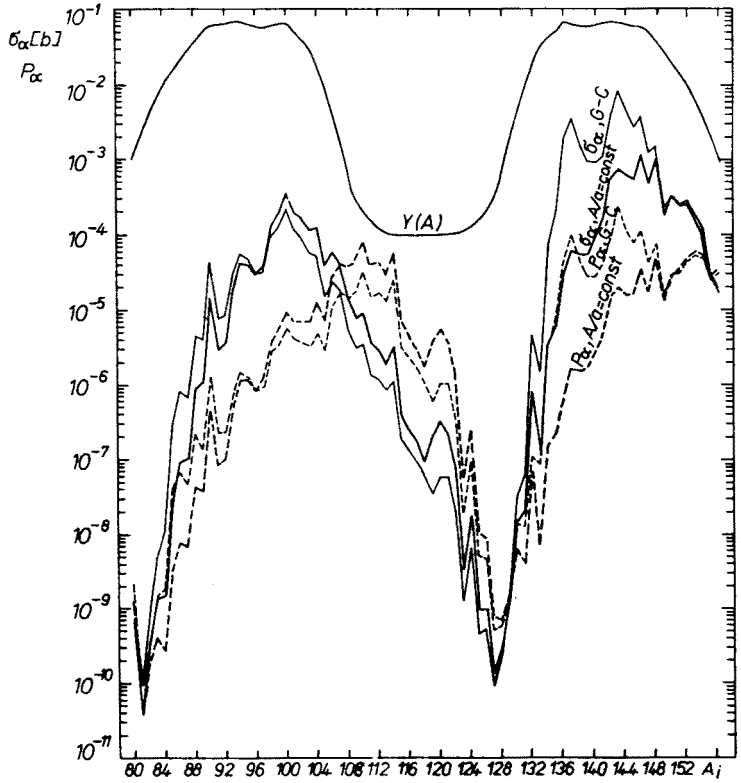

Fig. 10. The broken lines give the dependence of the α-emission probability (averaged over the charge distribution of fragments) on the fragment initial mass number. The cross-section for producing the α-evaporating fragments in the thermal neutron fission of ^{235}U as a function of fragment mass is given by solid lines. The bold curves were obtained under the assumption that A/a values are equal to 7 for the light fragments and to 9 for the heavy ones, the thin lines are the result of using the Gilbert-Cameron semi-empirical formula [14]. Note that the saw-toothed shape of the anticipated emission probability distribution is much more pronounced than in the case of neutron emission

The eventual error of the order of 15 per cent is tolerable in calculations of this kind, and is included in the overall error estimate.

2.4.4. Multiple emission. It is known that on the average more than one neutron is emitted from the fission fragment. The scheme of calculating the neutron multiplicity distribution is quite straighforward if the γ-ray competition is neglected.

From a total of N_0 fragments of the same charge and mass, $t_0 N_0$ fragments deexcite

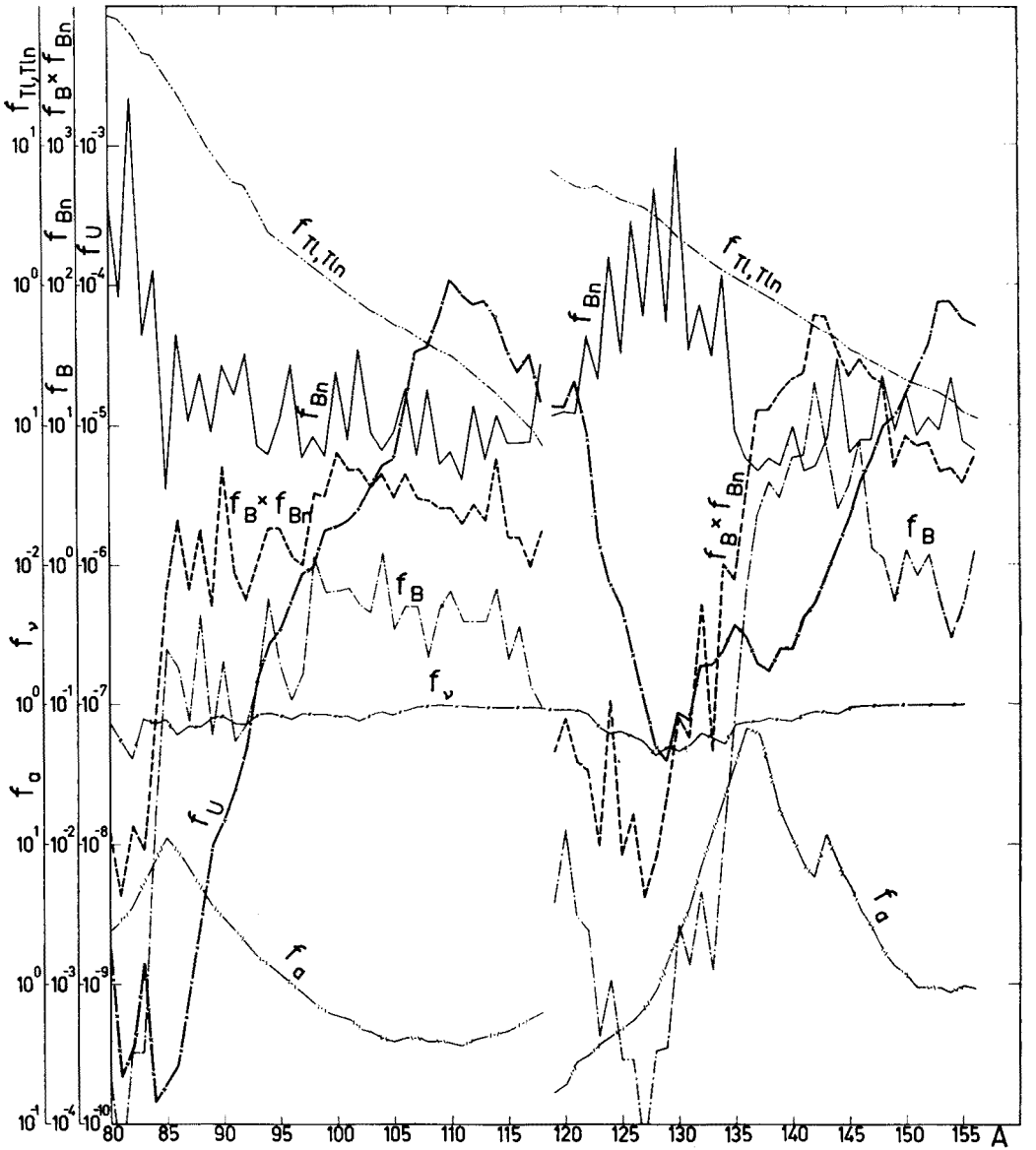

Fig. 11. The Γ_α/Γ_n ratio is approximately equal to the product of the displayed here f-functions. Note that almost all factors are rapidly varying with A; thus the maximum of the cross-section curve is, in a sense the result of "lucky" coincidence of the high values of all the factors. The discontinuity at $A = 118$ is due to that the f-functions have been separately defined for the L- and H-fragments (see Eq. (2))

through neutron evaporation, where

$$t_0 = \int_{Bn0}^{\infty} g_0(U)dU / \int_0^{\infty} g_0(U)dU$$

and $Bn0$ is the separation energy of a neutron from the parent fragment. Thus, the probability that no neutrons are emitted is $p(0) = 1 - t_0$. Let $R_n(U; U_r^n)$ be the emission rate of neutrons of energy $E_n = U - U_r^n - Bn$ from the fragments having an excitation energy

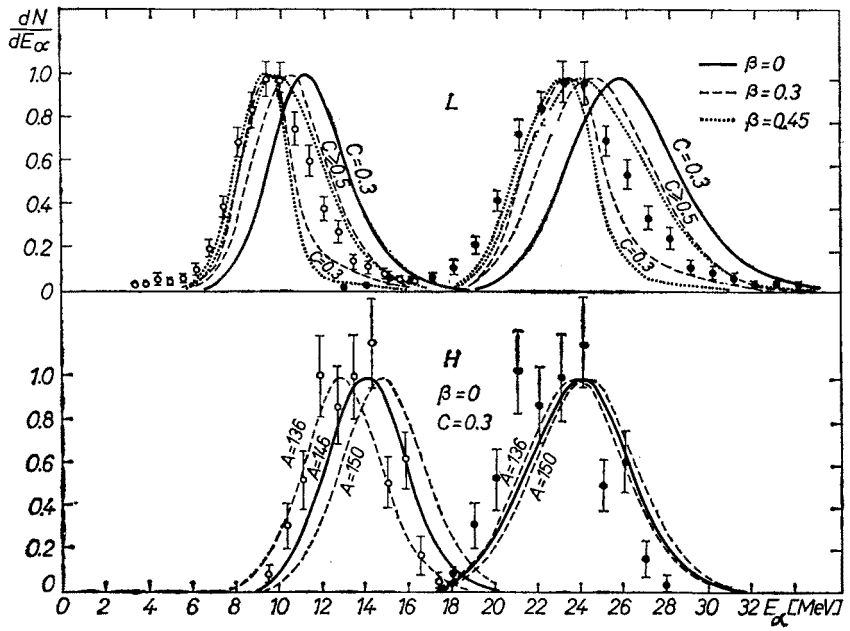

Fig. 12. The calculated spectra of particles emitted from the light fragments (upper part of the figure) and heavy ones. The spectra in the fragment reference system are on the left-hand side, results of the transformation to lab-system and experimental spectra are shown on the right. The dashed and the dotted curves in the upper part of figure are the results of taking account of the effects of deformation of the L-fragment. The letters β and c denotes respectively the deformation parameter and the moment of inertia of the residual fragments in the rigid body units

of U, (see Section 2.1). The $N_1 = t_0 N_0$ fragments will then have the residual energy distributed as:

$$g_{1n}(U_r^n) = \int g_0(U)\, R_n^1(U; U_r^n)\, dU.$$

In the second step of deexcitation the

$$N_2 = t_1 N_1 = \frac{\int_{Bn1}^{\infty} g_{1n}(U_r^n) dU_r^n}{\int_0^{\infty} g_{1n}(U_r^n) dU_r^n} \times N_1$$

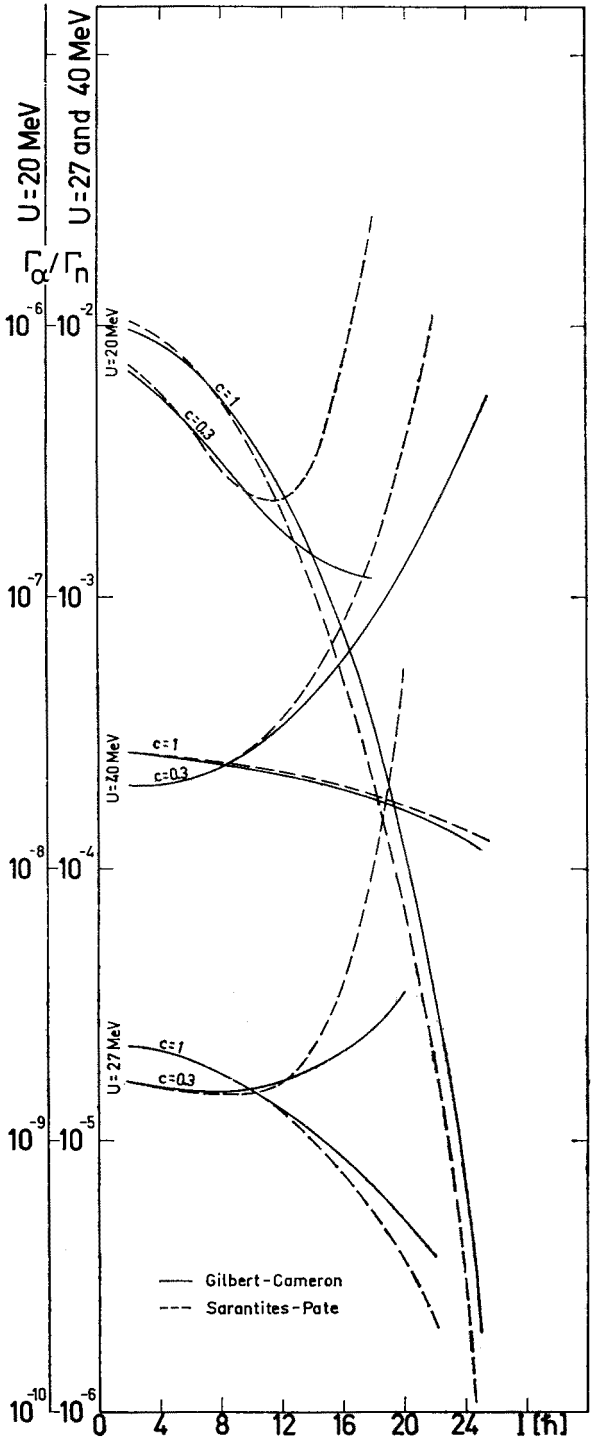

Fig. 13. Dependence of the Γ_α/Γ_n ratio on the initial spin of the light fragment for various initial excitation energies and moments of inertia. In addition the results of two methods of including the YL (yrast levels) effects into calculations are compared

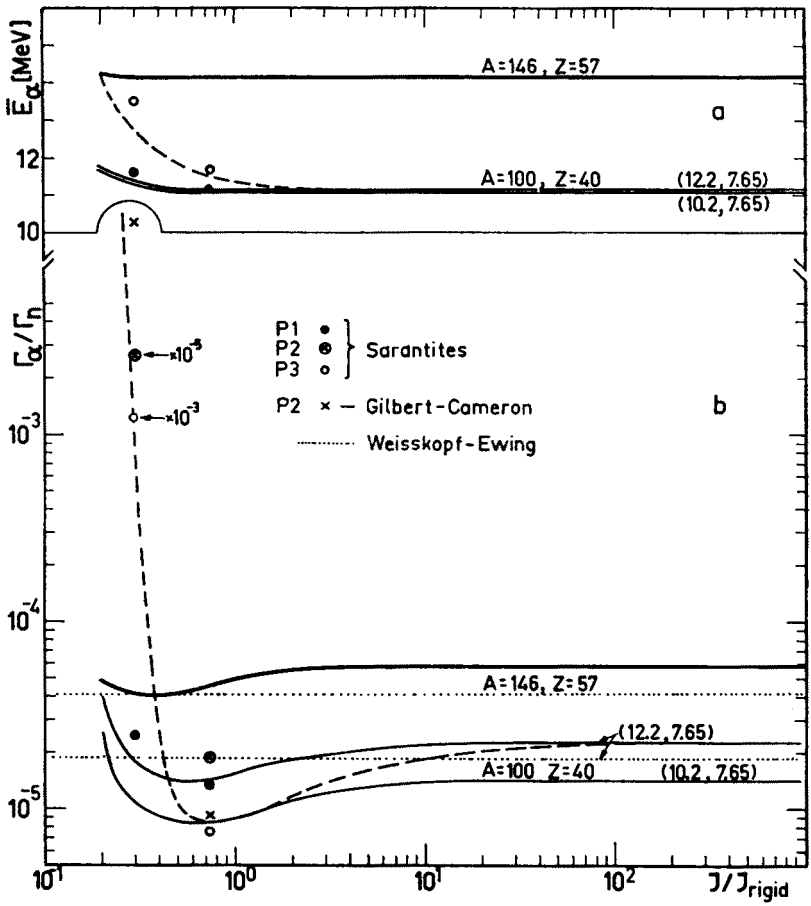

Fig. 14. Dependence of the mean kinetic energy of alphas (in the fragment reference system) (a) and of the Γ_α/Γ_n ratio (b) on the moment of inertia for the most probable α-emitting L- and H-fragments. The solid lines refer to the P1 initial spin distribution; results for P3 are given by dashed lines. Results of taking into account the YL effects by using the Sarantites-Pate method are also shown. For comparison the results of calculations based on the spin independent Weisskopf-Ewing formula are given. The numbers in parentheses refer to the Gaussian parameters $\bar{U}$ and σ of the excitation energy distribution $g(U)$

fragments deexcitate in this way, hence

$$p(1) = \frac{N_1 - N_2}{N_0} = \frac{N_1 - N_2}{N_1} \times \frac{N_1}{N_0} = (1 - t_1)t_0.$$

The new R and g distributions may now be calculated, *etc.* Similar calculations can be performed for the α-particles.

Fig. 15. The initial excitation energy distribution $g_0(U)$ and distributions of residual energy after the subsequent steps of deexcitation. These results concern the $A = 146$, $Z = 57$ nucleus. For the $A = 100$, $Z = 40$ nucleus the difference between the mean excitation energy before and after the first step of deexcitation is even smaller (of about 3 MeV)

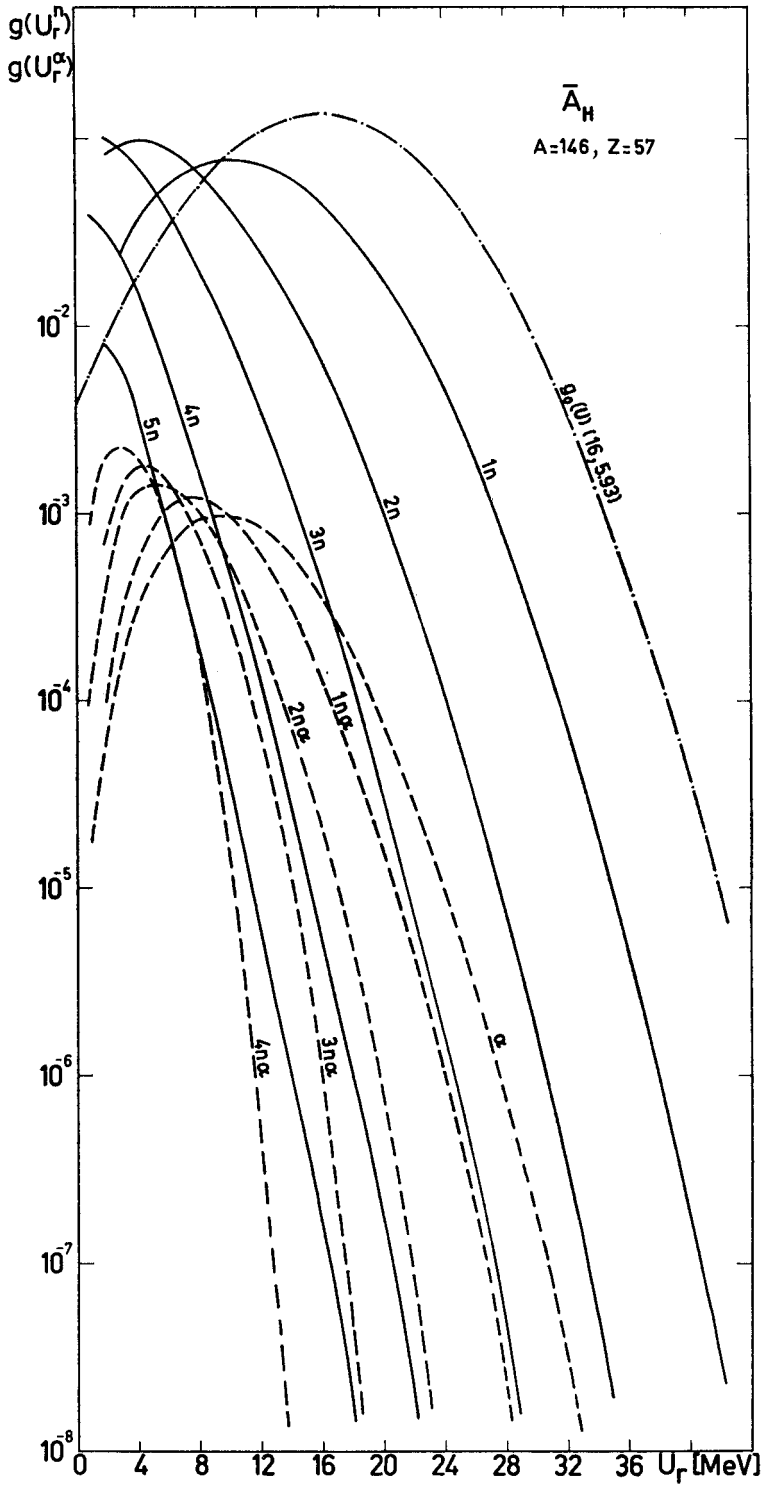
g(U_r^n)
g(U_r^α)
Ā_H
A=146, Z=57
g_g(U) (16,5.93)
1n
2n
3n
4n
5n
α
1nα
2nα
3nα
4nα
10^-2
10^-3
10^-4
10^-5
10^-6
10^-7
10^-8
0
4
8
12
16
20
24
28
32
36
U_r [MeV]

In the first step $N_{1\alpha} = (\Gamma_\alpha/\Gamma_n)_1 N_1$ fragments emit alpha particles, leaving the fragments at excitation energy U_r^α distributed as

$$g_{1\alpha}(U_r^\alpha) = \int g_0(U)\, R_\alpha^1(U; U_r^\alpha)\, dU.$$

In the second step alphas can be produced as a result of the subsequent α-deexcitation of these $N_{1\alpha}$ fragments ("2α-deexcitation") or α-emission from the above mentioned N_{1n} fragments ("$n\alpha$-deexcitation").

TABLE III

Scheme of the multiple emission calculations

Deexcitation step	1	2	3	etc
Cumulative probability of α-emission $\Sigma\alpha/N_0$	$(\Gamma_\alpha/\Gamma_n)_1\, t_0$	$(\Gamma_\alpha/\Gamma_n)_1\, t_0 + (\Gamma_\alpha/\Gamma_n)_2\, t_0\, t_1$	$(\Gamma_\alpha/\Gamma_n)_1\, t_0 + (\Gamma_\alpha/\Gamma_n)_2\, t_0 t_1 + (\Gamma_\alpha/\Gamma_n)_3\, t_0 t_1 t_2$	
Number of alphas	$N_{1\alpha} = (\Gamma_\alpha/\Gamma_n)_1 N_{1n}$ (neglected) $N_{2\alpha} = (\Gamma_\alpha/\Gamma_n)_2 N_{1\alpha}$	$N_{1n\alpha} = (\Gamma_\alpha/\Gamma_n)_2 N_{2n}$ (neglected) $N_{n2\alpha} = (\Gamma_\alpha/\Gamma_n)_3 N_{1n\alpha}$	$N_{2n\alpha} = (\Gamma_\alpha/\Gamma_n)_3 N_{3n}$	
N_0 of primary fragments				
Number of neutrons	$N_{1n} = N_0\, t_0$	$N_{2n} = N_{1n} t_1 = N_0\, t_0 t_1$	$N_{3n} = N_{2n} t_2 = N_0\, t_0 t_1 t_2$	
p (v)	$(1 - t_1)\, t_0$	$(1 - t_2)\, t_1\, t_0$	$(1 - t_3)\, t_2 t_1 t_0$	

The number of the former deexcitations is

$$N_{2\alpha} = (\Gamma_\alpha/\Gamma_n)_2 N_{1\alpha} = (\Gamma_\alpha/\Gamma_n)_1 (\Gamma_\alpha/\Gamma_n)_2 N_0$$

and even if $(\Gamma_\alpha/\Gamma_n)_2$ will be comparable with $(\Gamma_\alpha/\Gamma_n)_1$, the probability of such a process being negligibly small, as $(\Gamma_\alpha/\Gamma_n)_1$ is of the order of 10^{-5}. It may be interesting to note that $(\Gamma_\alpha/\Gamma_n)_2$ is really of the order of $(\Gamma_\alpha/\Gamma_n)_1$, although at first sight the cost of emitting of the α-particle ($\overline{E}_\alpha + B \approx 17$ MeV) excludes such a possibility. The reason for this apparently strange fact is that the alphas are most frequently emitted from the fragments excited to energies much higher than the average ones (see Section 4), and in effect the distribution of residual energy $g_{1\alpha}(U_r^\alpha)$ is only slightly shifted at lower energies with regard to the primary distribution $g_0(U)$, which is seen in Fig. 15.

Simultaneously through "$n\alpha$-deexcitation"

$$N_{1n\alpha} = (\Gamma_\alpha/\Gamma_n)_2 N_{2n} = (\Gamma_\alpha/\Gamma_n)_2 N_0 t_0 t_1$$

alphas are emitted. The residual excitation energy distribution can be calculated similarly:

$$g_{1n\alpha} = \int g_{1n}(U_r^n) R_\alpha^2(U_r^n; U_r^\alpha) dU_r^n$$

and the calculations may proceed in this way up to the point where the contribution of the subsequent evaporations will be negligible with regard to the previous ones. The relevant scheme of calculations is shown in Table III.

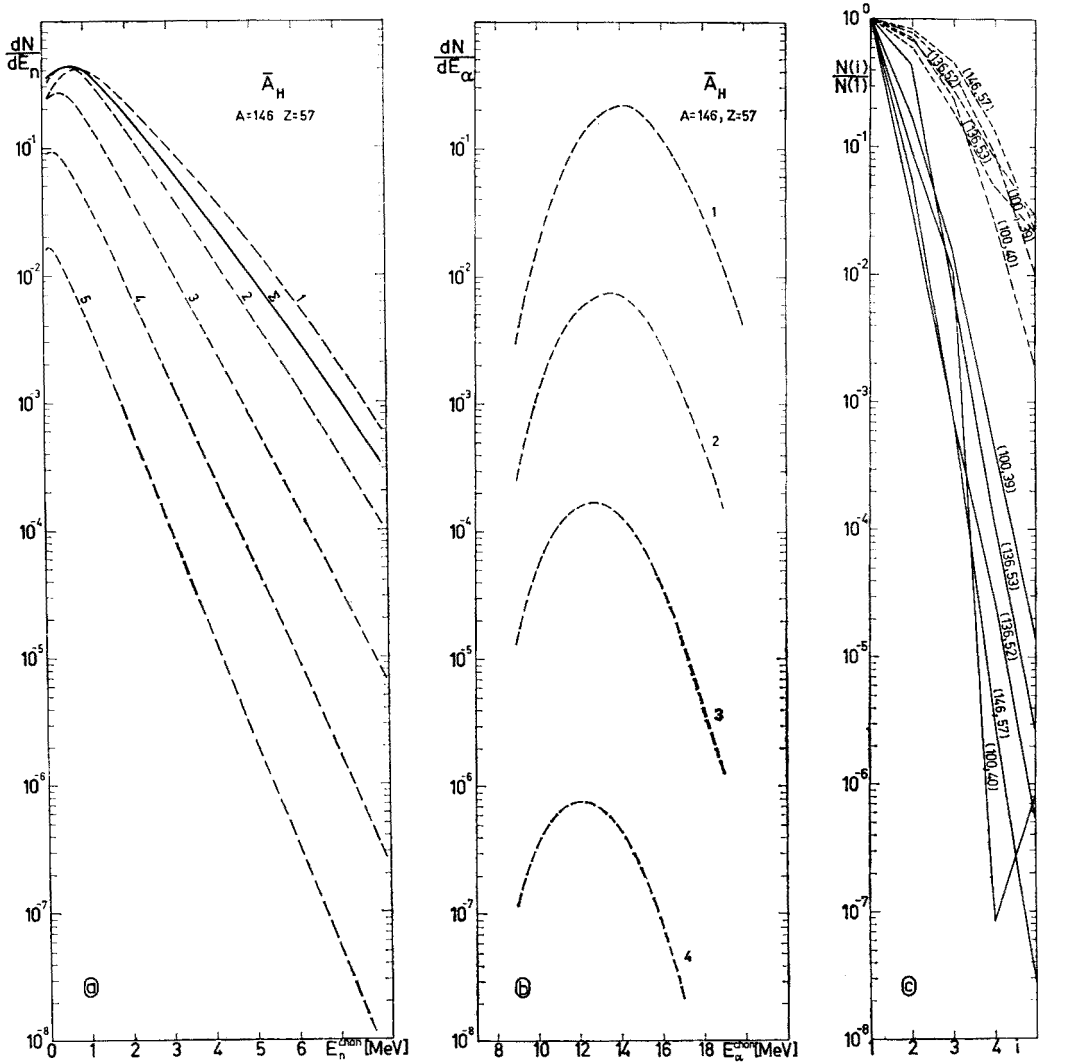

Fig. 16. a) The energy spectra of neutrons emitted in subsequent steps of deexcitation and the total spectrum normalized to the area of the first step spectrum. The importance of taking into account the fact of multiple emission is evident. b) Spectra of alphas from the α, $n\alpha$, $2n\alpha$ and $3n\alpha$ deexcitation processes. It may be seen that even if the contribution of the subsequent deexcitation steps would be greater, the total spectrum would not be drastically changed. c) Intensities of the subsequent deexcitations in comparison to the first one in the case of alpha (solid lines) and neutron (dashed lines) emission

In the course of calculations we have made two simplifying assumptions: (1) we have not accounted for the changes of penetrabilities and (2) nor provided for the changes of spin distribution $T(I)$ in the subsequent steps. The error of Γ_α/Γ_n connected with the first assumption is of about 10 per cent in every step (see Fig. 7). As regards the second assumption, we based on the results of Williams and Thomas [74], according to which the change of I in our case would not be more than $2\,\hbar$ in each step.

Energy distributions of neutrons and alphas evaporated are shown in Figs. 16a and 16b; contributions of the subsequent deexcitations as compared to the first one are shown for the case of neutrons and alphas in Fig. 16c.

It should be noted that latter results are strongly dependent on the B and Bn values in subsequent steps of the cascade, which in the case of the (100, 40) nucleus revealed itself as an upturning of the curve for alphas in Fig. 16c.

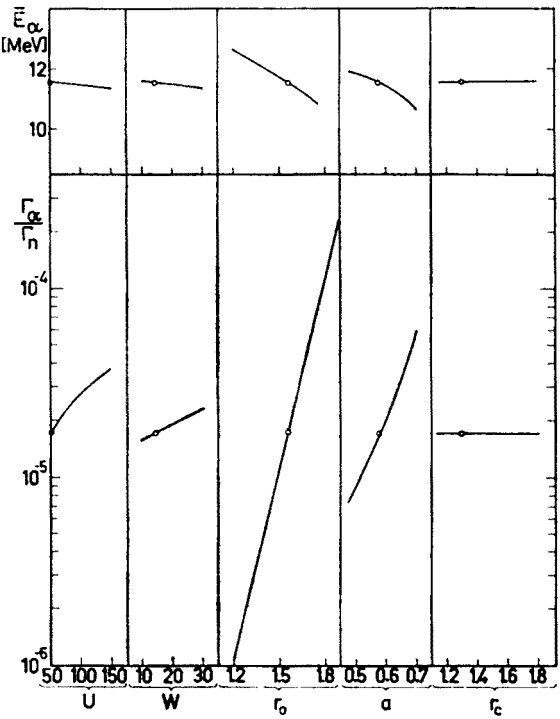

Fig. 17. Variation of the mean energy of α-particles (in the fragment reference system) and of the Γ_α/Γ_n ratio with the optical model parameters. The r_0 parameter is defined by the known relation $R = r_0 A^{1/3}$. The presented results concern the (100, 40) nucleus. Points mark the parameter values used

The following observations can be made regarding the taking into account of multiple emission:

(*i*) $\bar{E}_n$ in the fragment reference system is decreased by about 150–250 keV (or by 15–25 per cent) while $\bar{E}_\alpha$ is decreased by only 50–100 keV (0.5–0.7 per cent);

(*ii*) contrary to the situation in neutron emission, the probability of alpha emission is only slightly increased, by about 10 per cent.

2.4.5. Optical model parameters (OMP). The known deficiency of the statistical model is the necessity of knowing the inverse reaction cross-section (or T_l coefficients) *i.e.* cross-sections for particles incident on the excited nucleus, while the available optical model parameters refer to the interaction with nuclei in the ground states. This fact can influence the results, as it is presumed that the nucleus in excited state can be less transparent to

incident particles, because with increasing excitation energy the Pauli principle inhibits fewer transitions [5]. However, this effect should be responsible *e.g.* in the ^{27}Al (α, α') reaction, for an only 5 per cent increase of the cross-section for 20 MeV α-particles, as was estimated in Ref. [52] and it seems that for the heavier nuclei this effect is also not important.

Differences in the shape, radius and diffuseness of the nucleus in the ground and excited states are the next sources of uncertainties, although probably not very serious. The effect of thermal increasing of the radius seems to be small (of the order of one per cent [5]). The shape (the distribution of deformation) of the nuclei in the region of rare earth elements changes rather slowly with excitation energy in the range of 0–40 MeV (see Ref. [59]) but for nuclei produced in fission this problem has not been explored as yet.

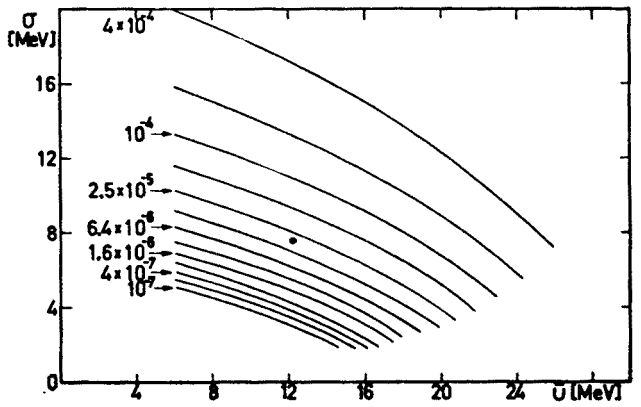

Fig. 18. The contour diagram giving the dependence of the Γ_α/Γ_n ratio on $\bar{U}$ and σ, the parameters of the Gaussian distributed excitation energy, in the case of emission from the (100, 40) nucleus. Point marks the parameter values actually used

Probably more important is the fact of using the OMP obtained from the experiments with the stable nuclei, although we deal with the fission fragments lying far from the β-stability line. Thus it was necessary to check the sensitivity of our results on the parameter uncertainties, the results being shown in Fig. 17.

It appeared that the dependence on the potential depths is not drastic and a serious error in this point seems to be rather improbable. On the other hand, changes in the geometric parameters r_0 and a can influence strongly both the intensity and energy spectra of α-particles. Unfortunately we have no data making possible serious error estimation in this case, and can only express the feeling that uncertainties involved in OMP should not falsify the Γ_α/Γ_n ratio by more than one order of magnitude. Sensitivity to r_0 suggests, however, that the question of deformation effects requires investigation (see Section 2.5).

2.4.6. Spin distribution and moment of inertia. Influences of these two factors are strongly interrelated. For low $c = J/J_{\text{rig}}$ values the Γ_α/Γ_n ratio rises rapidly for $I \gtrsim 14\ \hbar$ (Fig. 13) as then, owing to the spin dependence of the level density (see Eq. (3)), the low final spins are strongly preferred *i.e.* the transitions are preferred which have high $l \approx I$

values. Such transitions are possible for α-particles but not for neutrons. The result is that the P2 and P3 spin distributions give for $c \lesssim 0.3$ enormous α-intensities (very strongly dependent on the details of the high-spin tail of $T(I)$), but the energies of evaporated α-particles are then so high that these cases must be excluded when compared with experiment. On the other hand, when the moment of inertia is higher, the differences in Γ_α/Γ_n and $\bar{E}_\alpha$ are for various $T(I)$ and c values much smaller (see Fig. 14) making the problem of the choice of $T(I)$ and c of much lesser importance.

2.4.7. Other variables. Considerable sensitivity of the Γ_α/Γ_n ratio to the parameters of the $g(U)$ distribution is illustrated in a contour diagram (Fig. 18). Striking is the fact of the insensitivity of α-particle energies to the eventual errors in these parameters (Fig. 14a).

TABLE IV

Estimated uncertainties

	Separability	Yrast levels	γ	Multiple emission	f_ν		Optical model parameters	
a)	2.4.1.	2.4.2.	2.4.3.	2.4.4.	−10%	10%	2.4.5.	
b)	0.9—1.1	1.5	0.85	1.1	0.9	1.1	0.1	10
c)	∼0	$0 \lesssim \delta\bar{E}_\alpha^L \lesssim 0.3$	∼0	$-0.2 \lesssim \delta\bar{E}_\alpha^L < 0$	0		<2	>−2

	$c, T(I)$	$g(U)$				A/a		σ_z		B		Bn	
		$\bar{U}$		σ									
a)	2.4.6.	−2	+2	−2	+2	−1.5	+3	−0.05	+0.05	−1	+1	−0.5	+0.5
b)	0.4—1.5[d]	0.6	1.6	0.2	3.5	0.3	7	0.97	1.03	3	0.3	0.5	2.2
c)	$0 \lesssim \delta\bar{E}_\alpha^L \lesssim 2$	−0.02	0.02	−0.1	0.1	−0.5	0.6	∼0		0.06	−0.06	+0.06	−0.06

a) The estimated uncertainty of the parameter or section, where the problem is discussed.

b) The effect of the above uncertainty (or approximation) manifest itself by multiplying σ_α^L by the factor given in this line.

c) The error of $\bar{E}_\alpha^L$ related with this uncertainty (in MeV).

d) Actually these limits of intensity uncertainties are imposed by the rather conservative limit of increasing $\bar{E}_\alpha^L$.

Effects of the estimated uncertainties of other parameters as well as of those previously discussed on the calculated cross-section σ_α^L and $\bar{E}_\alpha$ (in the lab-system) are summarized in Table IV.

As it is seen, the disagreement between the calculated and experimental intensities of α-emission from the L-fragments could be explained only by combining several reasons. It should be noted, however, that a substantial improvement of the spectrum may be reached only by changing the OMP and especially the radius parameter r_0.

2.5. Deformation and evaporation

Looking for an explanation of difference between the behaviour of the H and L-fragments we paid attention to that according to calculations [29, 75, 76] as well as to the experimental results [77] the fragments in their ground states are deformed ($\beta \approx 0.25$–0.6) when $A \approx 100$, while the H-fragments are spherical.

The maximum of the evaporation spectrum is usually quite near to the Coulomb barrier, which on the other hand is considerably modified due to deformation and different for different points of the deformed nucleus. Thus it is intuitively evident that the shape of the nucleus can influence both intensities and spectra of the charged particles evaporated. Lowering of the barrier at the tips may be, however, more than compensated by its raising in other parts of the nucleus, thus the net result is difficult to forecast without detailed calculations. Several authors (see for example Refs [78, 79]) performed such calculations for the deep subbarrier case of α-decay. We tried to estimate the effect of deformation on evaporation as follows.

First of all we calculated the Coulomb potential $V_0^\theta(r)$ of the deformed nucleus. If the sphere of the radius $R_0 = r_c A^{1/3}$ is deformed into a spheroid, the semiaxes a and b can be determined from the relation

$$\frac{a}{b} = \frac{1+\beta}{1-\beta/2}$$

and from the volume conservation condition $\frac{4}{3}\pi R_0^3 = \frac{4}{3}\pi a^2 b$. The Coulomb potential inside and outside the spheroid can be calculated using the Swiątecki formula [80] after an apparantly typographical error corrected[1]. The nuclear potential $V_n^\theta(r)$ was generated for a given polar angle θ using the same optical model parameters as in the case of $\beta = 0$, changing only r_c and r_0. According to Ref. [25] for undeformed nuclei we have

$$r_0 = r_c\left[1+\left(\frac{3.46}{A}\right)^{1/3}\right]$$

and we supposed that this relation between r_c and r_0 holds for deformed nuclei also, only after replacing r_c by r_c^θ. This latter is easily obtainable from the equation of the spheroid. The sum of V_c and V_n for a couple of angles is presented in Fig. 19.

With the help of the ALA-4 program [24] we numerically solved for several angles θ the one-dimensional Schrödinger equation with the potential given by this sum. Using the penetrability coefficients $T_l^\theta(E_\alpha)$ obtained in this way we calculated the spectra and Γ_α/Γ_n ratios for these angles. Since we presume that the influence of deformation on neutron evaporation is of minor importance, we used the values of the neutron T_l known for undeformed nuclei. The next important assumption was that the solution of this essentially 3-dimensional problem may be obtained in the case of axial symmetry as a sum of

---

[1] The relevant equation should read:

$$L_2 = [\tfrac{1}{6}(\eta_0^3-\eta_0)\,Q_0(\eta_0) - \tfrac{1}{6}\eta_0^2] + [-\tfrac{1}{3} + \tfrac{1}{2}\eta_0^2 - \tfrac{1}{2}(\eta_0^3-\eta_0)Q_0(\eta_0)]\eta^2.$$

contributions from all the points of the nuclear surface, *viz.*

$$\frac{\Gamma_\alpha}{\Gamma_n} = \iint_S \frac{\Gamma_\alpha}{\Gamma_n}(S) f(S) dS \Big/ \iint_S dS = \int_0^{\pi/2} \frac{\Gamma_\alpha}{\Gamma_n}(\theta) f(\theta) \frac{dS}{d\theta} d\theta \Big/ \int_0^{\pi/2} \frac{dS}{d\theta} d\theta,$$

where $f(\theta)$ is the dependence of clustering probability on the site on the surface. We put $f(\theta) = 1$, which is equivalent to the simplest assumption (usually made in the statistical

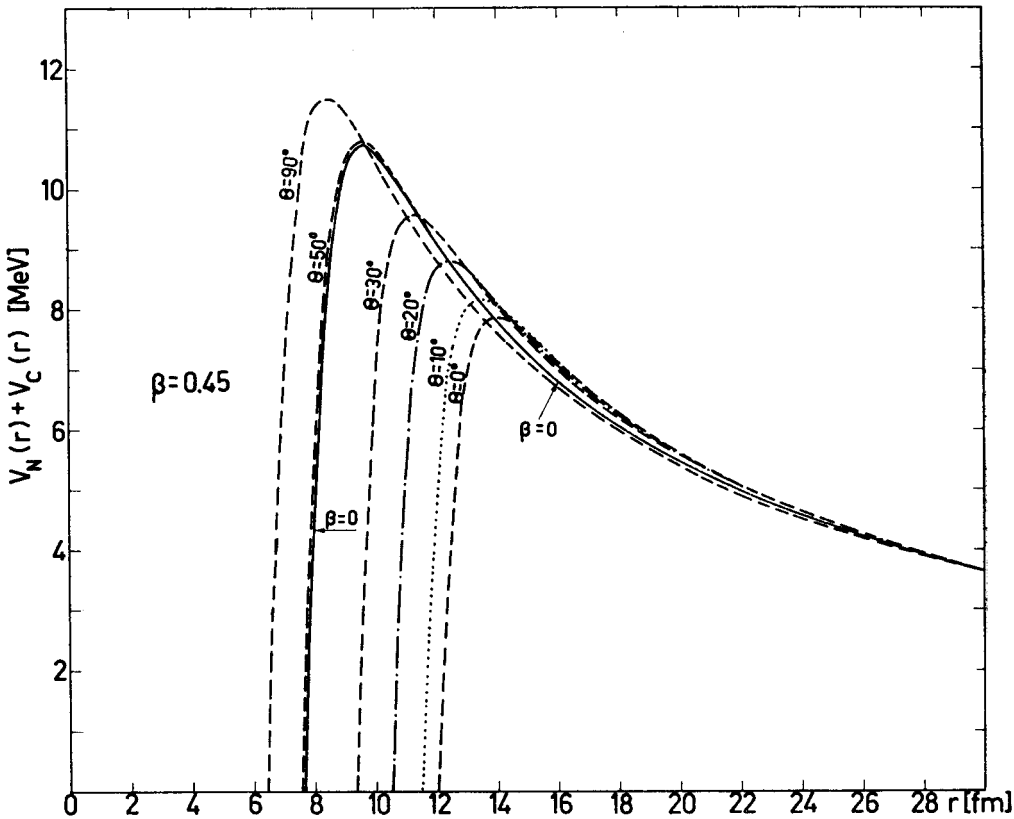

Fig. 19. The sum of nuclear and Coulomb potentials between the (100, 40) nucleus and an alpha particle at different polar angles. The deformation parameter β is equal to 0.45. For a comparison the potential of undeformed nucleus is shown also

model) that the α-particles are always present and "ready" to penetrate through the barrier. We then weight $\Gamma_\alpha/\Gamma_n(\theta)$ by a purely geometrical factor $dS/d\theta$, which for a spheroid is given by the equation

$$\frac{dS}{d\theta} = 2\pi a^2 b^2 \frac{\sin\theta}{a^2\cos^2\theta + b^2\sin^2\theta}.$$

Every other choice of $f(\theta)$ will result in decreasing the alpha emission intensity, although the spectrum can be modified (in both directions) within limits given in Fig. 20.

It appeared that for $c = 0.3$ the α-emission is strongly peaked at about $\theta = 10°$ (Fig. 22) and the resulting energy spectrum is very narrow (Fig. 12). With increasing c the spectrum of alphas rapidly widens as the predominating role of the low-angle α-particles decreases and the alphas from other angles (Fig. 20) begin to give more comparable contributions. However, even for $c = 0.75$ the spectrum is clearly lowered with regard to the case of undeformed nucleus, and the agreement with experiment seems to lie in the limits of the estimated systematic error of 1 MeV.

The question of α-emission intensity remains nevertheless open as a substantial increase of σ_{calc} is critically dependent on several not very well known factors. The calcula-

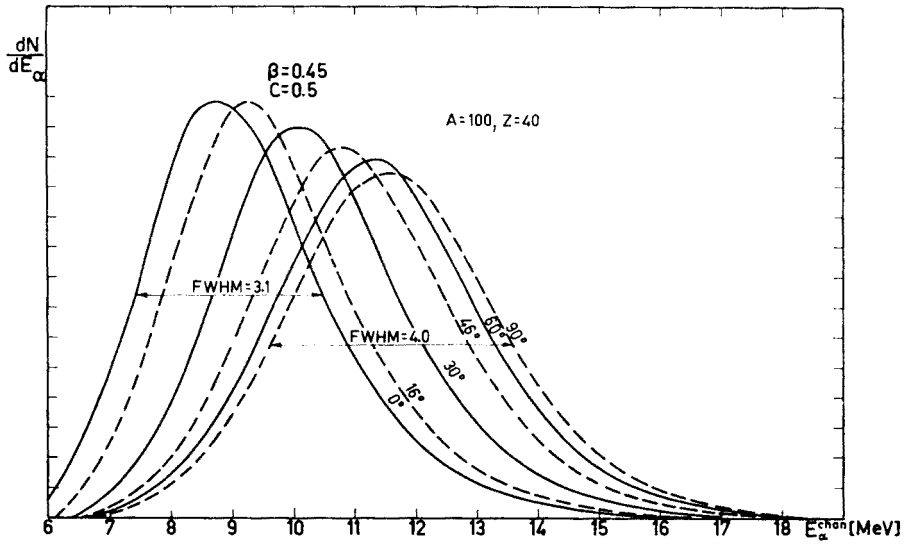

Fig. 20. Spectra of α-particles emitted from various points (denoted by polar angles) of the (100, 40) deformed nucleus

tions showed that while for $c = 0.3$ the increase of the intensity of α-emission (due to deformation) is 10-fold for $\beta = 0.45$ and 3-fold for $\beta = 0.3$, for $c = 0.5$–0.75 the intensity is even decreased by 15–20 per cent. Moreover, the increase of intensity for $c = 0.3$ is due almost entirely to the transitions with the highest angular momenta and so to the highest spins in the $T(I)$ distribution and to the yrast level effects. Thus the result is extremely sensitive both to the shape of $T(I)$ and on the way in which the YL's are included into the calculations. In fact, when the calculations are performed with the level density formula of Sarantites and Pate (see Section 2.4.2), the Γ_α/Γ_n ratio is increased not 10 times but about 200 times. In this case, however, our approximation $\Gamma_{tot} \approx \Gamma_n \gg \Gamma_\alpha$ becomes invalid (see Fig. 23) and it is necessary to account for the γ-ray deexcitation channel.

There is another possibility of increasing the calculated intensity of α-emission. When the nucleus is deformed ($\beta = 0.45$) and the initial spin distribution is not P1 but P3, then even for $c = 0.6$ the Γ_α/Γ_n ratio is increased 10-fold (for $c = 0.55$ as much as 60-fold).

The spectrum of alphas is then similar to that in the case of P1 spin distribution, $c = 0.5$ (see Fig. 12). Thus one should choose between the surprisingly low value of c and the high initial spin of the fragments.

3. *Angular distribution*

Data analysis described in Ref. [2] has shown that the strong anisotropy of polar alphas exists not only in the lab-system (owing to emission from the fragments in flight).

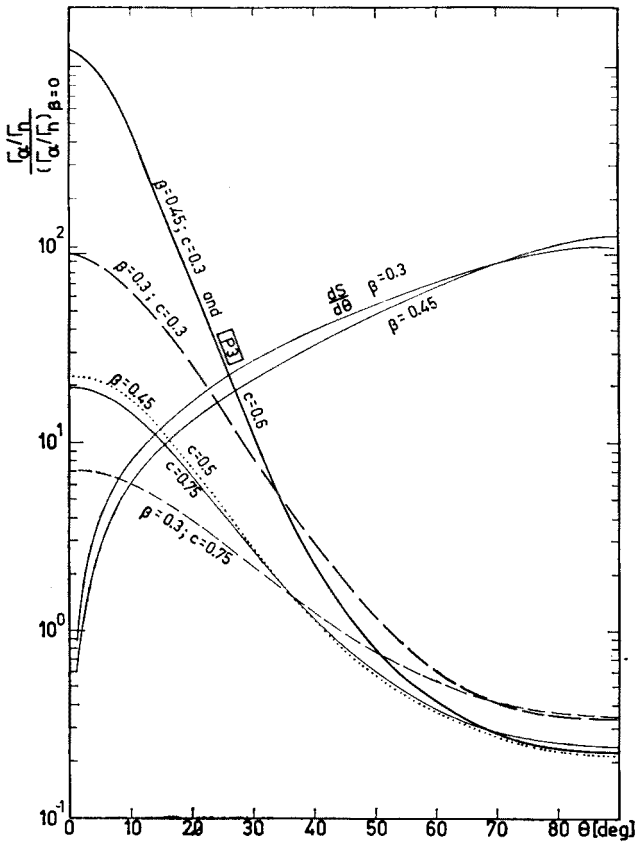

Fig. 21. The increase of the Γ_α/Γ_n ratio for the (100, 40) deformed nucleus with regard to the case of $\beta=0$, P1, $c = 0.3$ as function of the polar angle θ. All curves, except for the marked one, were calculated using the P1 spin distribution. The geometry factor $dS/d\theta$ is shown also. Note that for the equatorial angles the intensity of emission is actually diminished

but also in the center-of-mass of the fragment + alpha particle system. There can be at least three reasons of such an anisotropy:

(*i*) angular momentum of the emitting fragment

(*ii*) dependence of the barrier on the angle (due to deformation)

(*iii*) dependence of the clustering probability on the angle.

The theories referring to the first reason, based on the statistical model, were elaborated by Douglas and MacDonald [81], Liggett and Sperber [82], and by Ericson and Strutinski [5]. The first two approaches, being more exact, need 10^3–10^4 more computer time than the third one, thus being absolutely prohibitive for us. The results of comparison of the first and third method, done in Ref. [83], are however quite encouraging.

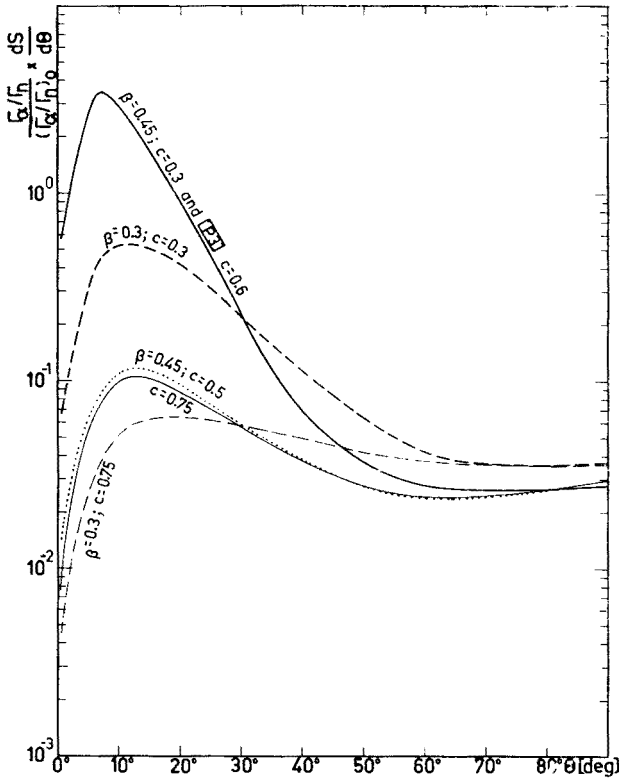

Fig. 22. Results of weighting of the $(\Gamma_\alpha/\Gamma_n)(\theta)$ values from Fig. 21 by the geometry factor $dS/d\theta$. The area under the curve gives the gain factor of the intensity of α-emission from the deformed nucleus as compared with spherical one

It lies in the spirit of statistical model that the angular distribution is determined by the phase space. Since the maximum level density occurs for the minimum value of the final spin (Eq. (3)), the emission of particles with the orbital angular momentum parallel to the initial spin of the nucleus is preferred. Thus the linear momentum is peaked in the equatorial plane, and since the angular momentum of the fragment is predominantly perpendicular to the fission axis [36, 69] the resulting distribution of emitted particles should be forward-backward peaked.

According to Ericson and Strutinski the angular-energy distribution of the emitted

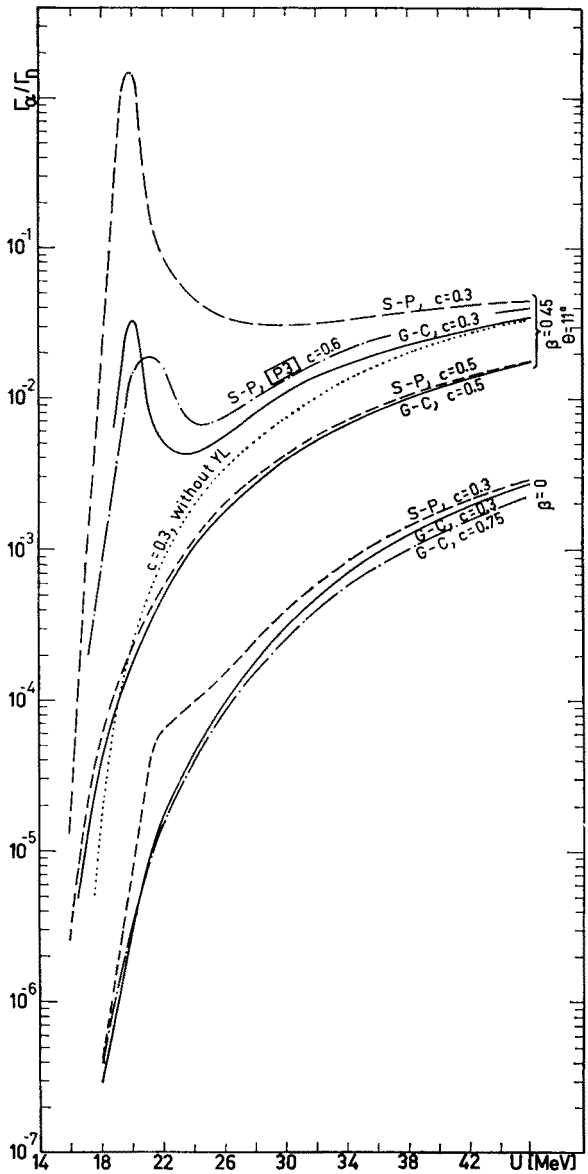

Fig. 23. Influence of deformation on the dependence of the Γ_α/Γ_n ratio on excitation energy. The peak at about 20 MeV is due to the YL effects. The letters $G-C$ and $S-P$ refer to the methods of including the YL's into the calculations (see Section 2.4.2)

alpha particles is given by

$$N(\theta, E_\alpha) = \int g(U) \sum_I T(I) \times$$

$$\times \frac{\Omega(U_r^\alpha, I = 0) \exp\left(-\frac{I^2}{2\sigma_\alpha^2}\right) \sum_l l T_l(E_\alpha) \exp\left(-\frac{l^2}{2\sigma_\alpha^2}\right) \omega_{Il}(\theta, E_\alpha)}{\sum_p \int dE_p \Omega(U_r^p, I = 0) \exp\left(-\frac{I^2}{2\sigma_p^2}\right) \sum_l l T_l \exp\left(-\frac{l^2}{2\sigma_p^2}\right) j_0\left(\frac{iIl}{\sigma_p^2}\right)}, \quad (7)$$

where

$$\omega_{Il} = \frac{1}{4\pi} \times \frac{\sum_k (-)^k (4k+1) \left[\frac{(2k)!}{(2^k k!)^2}\right]^2 j_{2k}\left(\frac{iIl}{\sigma_\alpha^2}\right) p_{2k}(\cos\theta)}{j_0(iIl/\sigma_\alpha^2)}.$$

Here j_0 and j_{2k} are the spherical Bessel functions, and the sum in the denominator runs over all deexcitation channels. As in Section 2.1 we substituted this sum by the neutron evaporation channel. It should be reminded that σ^2 is dependent on residual energy, as $\sigma^2 = cJ_{\text{rig}}T/\hbar^2$ (see Section 2.2.5). During the data analysis we assumed that in the center-of-mass the shape of the angular distribution is given by Eq. (7) and we varied the moment of inertia looking for the minimum of χ^2 (Ref. [2]). For simplicity we assumed that the value of c is the same for both the L- and H-fragments. The resulting angular distribution $W(\theta) = \int W(\theta, E_\alpha)\, dE_\alpha$ is shown in Fig. 24.

The dependence of $W(90°)$ on the moment of inertia is shown in Fig. 25. This result can hardly be considered encouraging, since the low value of c needed for explaining the

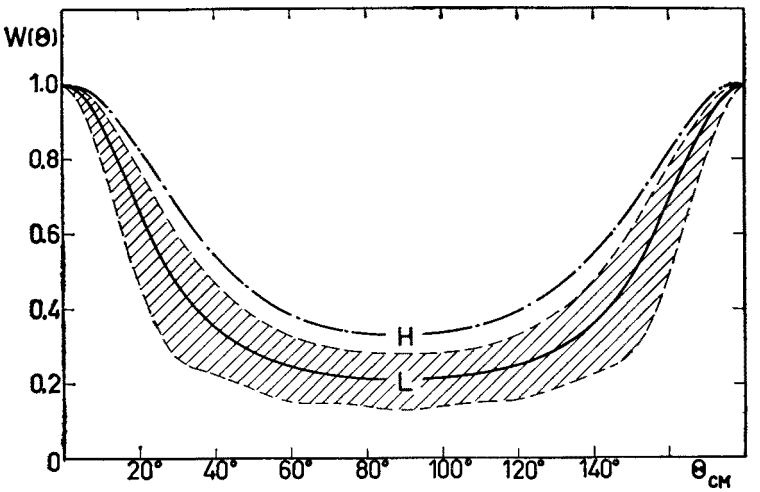

Fig. 24. The angular distribution of α-particles in the center of mass of the α+fragment system. This is a result of fitting the Ericson-Strutinski distribution (Eq. (7)) to the experimental data by varying the moment of inertia. The hatched area gives the statistical error. The distributions of alphas emitted from the L- and H-fragment were obtained by assuming that $c = J/J_{\text{rig}}$ values are the same for both the fragments

experimental result seems to be improbable. When using in calculations realistic values of parameters, the anisotropy $W(0°)/W(90°)$ is abour 3.5 times smaller than the experimental value of 5.7 ± 2.

It should be noted here that for such a low value of c the method of Ericson and Strutinski should not work [5], strictly speaking, but it appeared that at least the energy spectra and the Γ_α/Γ_n ratio are in very good agreement with the results of standard calculations described in Section 2.1.

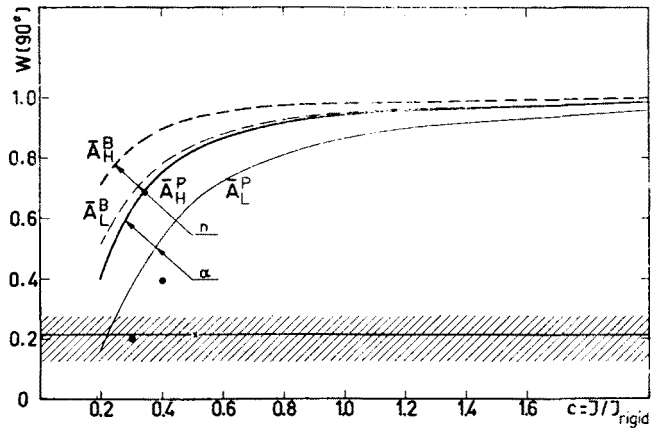

Fig. 25. The value of $W(90°)$, or the reciprocal of anisotropy of the neutron and the α-particle emission as a function of $c = J/J_{rig}$ calculated according to the Ericson-Strutinski method. Results are given for the most probable fragments in polar and binary fission. The experimental result and its statistical uncertainty (the hatched area) are shown also. The points give the results of approximate accounting for the deformation of the light fragment ($\beta = 0.45$ was assumed). The cross marks the result of calculation for $\beta = 0.45$ and initial spin distribution P3, all the other calculations were done using the P1 distribution

We have checked that the calculated angular distribution is only slightly dependent on all the relevant variables except the moment of inertia, and the result is from this point of view significant. On the other hand, although there are known measurements which give a low value of c (*e.g.* $c = 0.3$ for the ^{92}Mo (n, α) reaction with 14.5 MeV neutrons [84]), the predominating number of works for instance Refs [52, 82, 85, 86] show that at residual energy which is the most probable after α-emission (Fig. 15) the moment of inertia of fragments should be nearer to the rigid body value.

It may be argued, moreover, that even if one supposes that the moment of inertia of the fragment has, for unknown reasons, really such a low value, it should manifest itself in angular distribution of fission neutrons, while as it is known [6,7], anisotropy in this case does not exceed (in cms) a few per cent. This argument is not as strong as it looks, as already Bodansky [51] called attention to the fact that anisotropy especially of alpha particles often greatly exceeds the rigid body predictions. As an example can serve the great anisotropy of alphas in the (n, α) reactions measured in Ref. [87] and analyzed in Ref. [81].

The reasons of this phenomenon remain unexplained, but it should be stressed that the method used here does not take into account the yrast effects. Inclusion of these effects

into calculation should reduce the intensity of transitions with lowest l values giving the least anisotropic contributions, thus the calculated anisotropy should increase.

Moreover, no one of the methods cited [5, 81, 82] takes into account the effects of the second and third points given at the beginning of Section 3. We have tried to use the T_l coefficients calculated for a deformed nucleus which increased somewhat the calculated anisotropy (Fig. 25), but it is obvious that a more fundamental approach to this subject is needed.

4. On the sharing of the energy released in fission

It was already mentioned in Section 2.2.7a that the energy released in the fission process, which is uniquely determined for the fixed mass and charge ratio of the fragments is shared between the kinetic and excitation energies of the fragments. All these quantities are widely distributed, but the data on correlations between these distributions are scanty. It seems that the polar emission phenomenon (if our understanding of its nature is correct) offers some possibilities in this context.

Let us denote by $\bar{E}^{*p(b)}_{H(L)}$ the average kinetic energy of the $H-$(or $L-$) fragment in polar emission (or in binary fission); the asterisk detones the pre-emission value.

The mean total kinetic energy of binary fission fragments with the masses $A_L = 100$, $A_H = 136$ is equal to 176.3 MeV [17]. In the case of polar emission from the L-fragment it appeared [1] that

$$\bar{E}_{\text{tot}} = \bar{E}^{*p}_{H} \frac{A_L + A_H}{A_L} = \frac{236}{100}(69.8 \pm 1) = (164.1 \pm 2.4)\ \text{MeV}$$

i. e. is by $\Delta E_{\text{kin}} = (12.2 \pm 2.4)$ MeV smaller. The mean total excitation energy of the fragments is in this case higher than normally by the same value. On the other hand one can calculate the distribution of this energy for the α-emitting fragments as

$$\frac{\Gamma_\alpha}{\Gamma_{\text{tot}}}(U) \times g(U) \approx \frac{\Gamma_\alpha}{\Gamma_n}(U) \times g(U),$$

and the result (Fig. 26) shows that on the average the excitation energy of the L-fragments should be greater by $\Delta U = U^p_L - U^b_L \approx 16$ MeV than in the usual binary fission. The picture looks now as follows: when the excitation energy of the light fragment increases by about 16 MeV, 75 ± 20 per cent of it is supplied at the cost of the kinetic energy, and only the balance, $(16 \pm 1) - (12.2 \pm 2.4) = (3.8 \pm 3)$ MeV is taken from the heavy fragment. In other words, $\Delta \bar{U}_H / \Delta \bar{U}_L = -0.24 \pm 0.18$.

These figures can be modified due to the YL effects in deformed light fragments (Fig. 23): the mean excitation energy of the L-fragments emitting polar alphas would be then smaller than in spherical nuclei, *viz.* of the order od 23 MeV. Then $\Delta \bar{U}_H / \Delta \bar{U}_L = 0.2 \pm 0.24$, thus in this case the conclusion that the excitation energy of the L-fragment is increased mainly to the cost of kinetic energy is even more convincing.

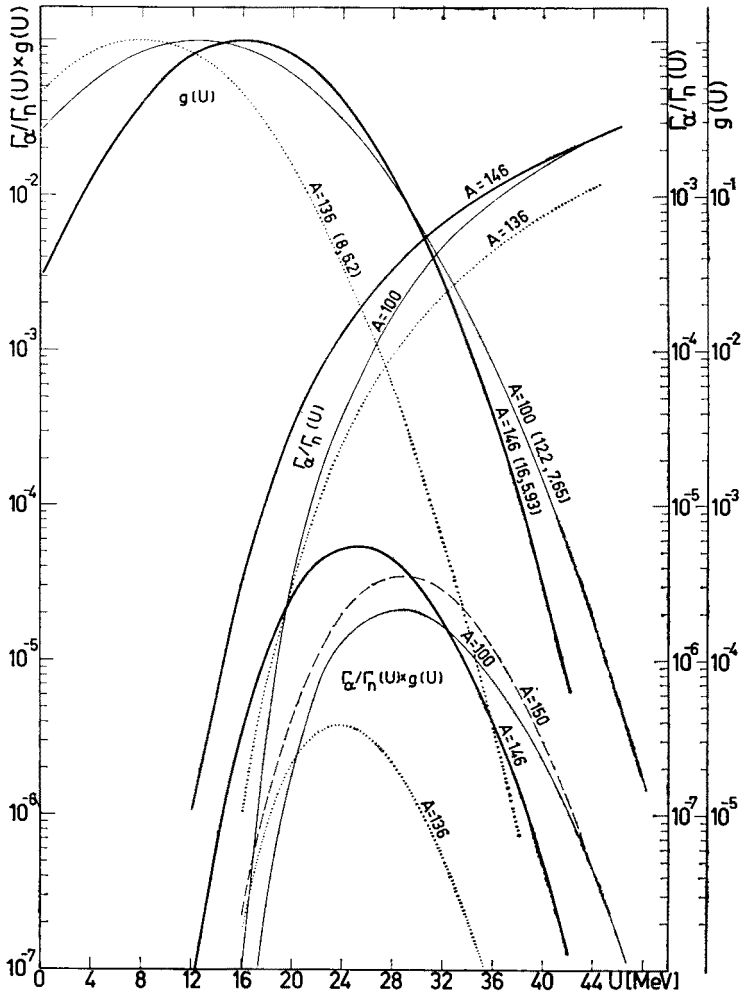

Fig. 26. The excitation energy distribution of the α-emitting fragment is given by the product of the excitation energy distribution of the binary fission fragments $g(U)$, and the probability of alpha emission as a function of U, approximately given by $(\Gamma_\alpha/\Gamma_n)(U)$. Note that significant α-particle evaporation occurs from the fragments excited by about 15 MeV higher than usually

Similar considerations for the case of polar emission from the heavy fragments should in principle be more reliable due to the better agreement of calculations with experiment. Unfortunately the determination of $\overline{E}_L^p$ was in this case more difficult, thus $\overline{E}_{\text{kin}}$ is less accurate: (-6.6 ± 4) MeV and $\Delta\overline{U}_L/\overline{U}_H = 0.27\pm0.44$, which anyway is in accordance with the above conclusion.

The $\Delta\overline{U}_L/\Delta\overline{U}_H$ and $\Delta\overline{U}_H/\Delta\overline{U}_L$ ratios are averaged over the total kinetic energy distribution, thus further measurements (see Section 5.4) are needed to provide more detailed conclusions on sharing of the energy released in fission.

We should like to stress that the polar emission plays here the role of a probe only, by using which we can learn what happens with the excitation energy of one fragment of the (normal, binary) fission, when the energy of the other increases.

5. Proposed methods of verifying the evaporation hypothesis

5.1. Repeating of the above measurements

The accuracy of the first experiment on polar emission is not spectacular. Especially the angular distribution of polar alphas may be biased by unknown systematic errors. Thus, before engaging into a more advanced theoretical analysis of the above results there is a bad need of repeating such measurements. Use of the position sensitive detectors would ease substantially the data analysis, improving angular resolution and the statistics.

Much easier would it be to obtain more precise energy spectra of the alphas emitted along the fission axis as well as of the fragments, which is needed to conclude as to the significance of divergencies between the experimental and calculated spectra.

5.2. Other fissioning nuclei and excitation energies

Results of both kinds of experiments are relatively easy to predict in the framework of the hypothesis considered.

In particular, it is known from experiments on fission induced by neutrons of various energies [88] that almost all the excitation energy of a fissioning nucleus which is above the threshold goes to the excitation of fragments. On the other hand the excitation energy dependence of the calculated probability of the polar emission is strong enough (Fig. 18) to be observed experimentally.

Quite recently were published results of experiment done by Rajagopalan and Thomas [89], who in the fission of ^{238}U by 42 MeV protons observed the effect reminding the polar emission, while at 16 MeV the effect was much weaker.

5.3. Other particles

We have performed calculations of spectra and of the evaporation probabilities of p, d, t, ^{3}He and ^{6}He. Since the calculations were performed for only 30 pairs of (A, Z) for every particle, we did not use the approximation (2), but calculated $\Gamma_{\text{part}}/\Gamma_{n}$ and the spectra directly from the Eq. (1), taking account of the spins of these particles.

All the relevant distributions and parameters were used such as in the calculations of the α-particle evaporation, of course with the exception of the optical model parameters (OMP) and separation energies. The latter were taken from the tables of Garvey *et al.* [16]; references regarding the OMP used are given in Table V, where the calculated ratios of intensities polar particles/polar alphas [%] are given. Results of averaging of the calculated cross-sections over the fission fragment charge distribution are shown in Fig. 27. For estimating the ratios of intensities we have used the linear interpolation and extrapolation in the logarithmic scale of the figure, which should be accurate within $\pm 50\%$.

Larger uncertainty may be caused by the fact that the precise reason for discrepancy between the calculated and the measured intensity of alpha emission from these frag-

ments is unknown. If this discrepancy is due to the deformation, then the ratios polar particles/polar alphas should be smaller, since it appeared that particles other than alphas are much less succeptible to this effect. The deformation $\beta = 0.45$, producing a 10-fold increase of alpha particle intensity (in the case of $c = 0.3$ and the P1 spin distribution), causes only a 2-fold increase of ^{6}He intensity. The cross-section for producing fragments deexciting through proton and triton emission is for a deformed nucleus even smaller, by 30 and 20 per cent, respectively, as compared with the spherical one.

Although these ambiguities are disappointing, the accuracy of the above estimations seems to be sufficient to forecast that, *e.g.*, ^{6}He would be practically absent at extreme angles, while in normal tripartition they are present in easily measurable quantities [95].

TABLE V

The calculated intensities of some light particle evaporation and the sources of the OMP used

Particle		p	d	t	^{3}He	^{6}He
polar particles / polar alphas [%]	*L*	31	4	8.6	4×10^{-5}	3.3×10^{-3}
	H	14	1.6	2	6×10^{-7}	1.2×10^{-3}
References		[88]	[89][a]	[90]	[90][b]	c

[a] Perey's parameters (see Ref. [92]) or OMP given in Ref. [93] give the same results within the limits of ±20 per cent.

[b] OMP given by Hodgson in their recent book [94] result in about five times smaller cross-sections.

[c] Since the OMP for the interaction of ^{6}He with nuclei are not known, we assumed that the depths of the real and imaginary potentials are the same as in the case of alpha emission, but r_0 was taken $1.17[1+(6/(A-6)^{1/3}]$, not $1.17\,[1+(3.56/(A-4)^{1/3}] \approx 1.17\,[1+(4/(A-4)^{1/3}]$ as for alphas [25]. This increased the r_0 value from 1.55 to 1.62 in the case of emission from the $A = 100$ nucleus.

Probably a more convincing test of the evaporation hypothesis will be the measurement of other particle spectra. As calculations have shown (Fig. 28), the evaporated particles, especially tritons, would appear in a very convenient energy range from the experimental point of view.

For transformation to the lab-system (we performed it for the mean laboratory angle of observation of 12.5° with respect to the fission axis, which was typical for our experiment) the knowledge of the kinetic energy of the fragments before emission was needed. We found it assuming that the difference between the initial excitation energy of the "normal" fragment and that, which deexcites by emitting some charged particle, $\Delta U = U^p - U^b$ is in 75±25 per cent supplied by the total kinetic energy, like in the case of the alpha particle emission. The uncertainty given entails quite small shifts of the calculated spectra, between 0.03 MeV for protons and 0.2 MeV for ^{6}He.

Fig. 27. Dependence of the cross-section for producing in the thermal neutron fission of ^{235}U the fragments emitting various charged particles on the mass number of the fragments. The A/a value was assumed as 7 for the light and 9 for the heavy fragments

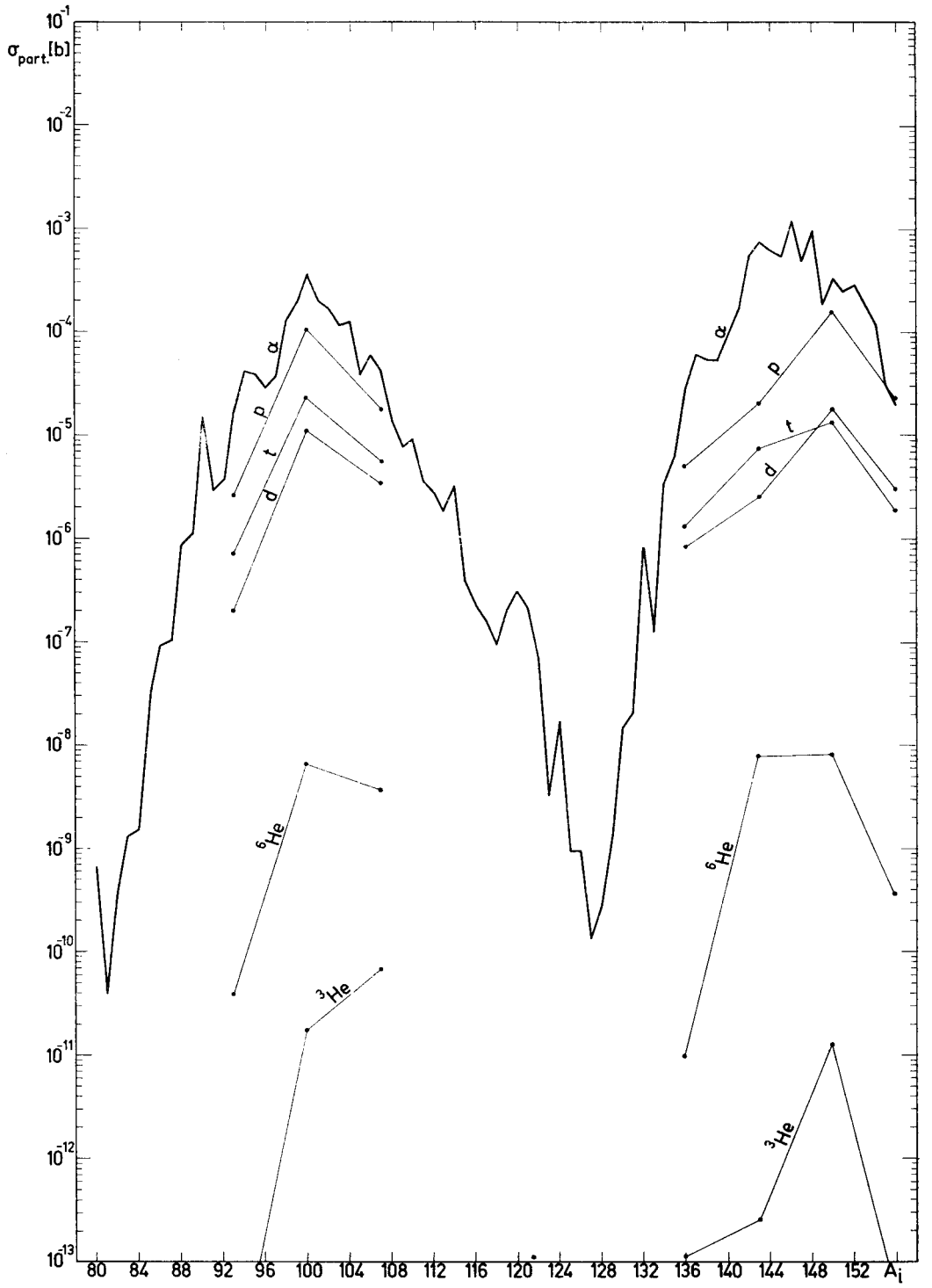
σpart. [b]
10-1
10-2
10-3
10-4
10-5
10-6
10-7
10-8
10-9
10-10
10-11
10-12
10-13
80 84 88 92 96 100 104 108 112 116 120 124 128 132 136 140 144 148 152 Ai
α
p
t
d
6He
3He
α
p
t
d
6He
3He

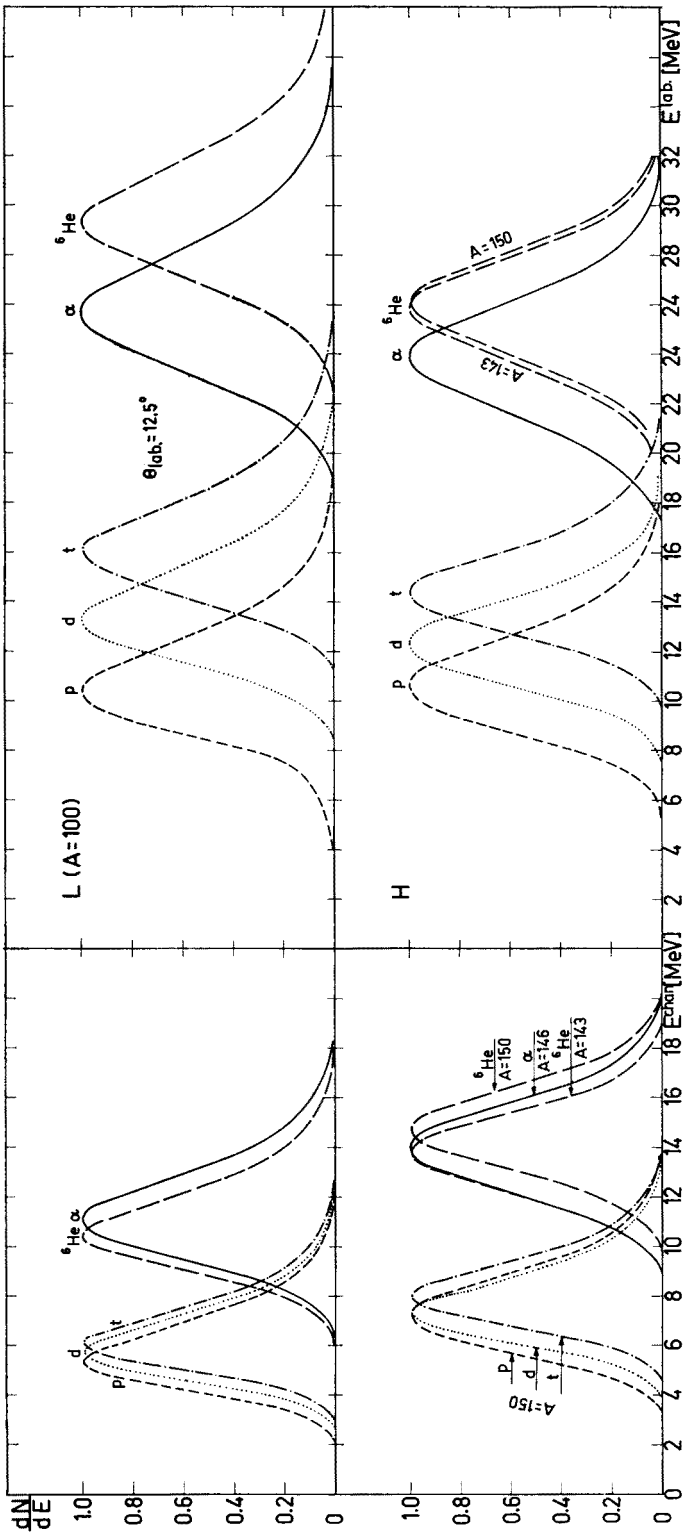

Fig. 28. Spectra of various charged particles evaporated from the fragments. The deformation was not taken into account (*cf.* also caption to Fig. 12)

5.4. The $\alpha-f-f$ experiment

An experiment in which event-by-event energies of both the fragments and of the polar alphas are registered offers the possibility of verifying the mass yield calculations (Fig. 10). Moreover, it will make possible more detailed insight into the interesting problem of the correlation between the excitation energies of both the fragments. Especially one can exploit the fact that different evaporated particles "probe" different excitation energies (see Fig. 29).

6. Conclusions

We proposed a hypothesis that the "polar emission" phenomenon [1, 2] is the result of in-flight deexcitation of the fragments through α-particle evaporation.

Basing on the statistical model of deexcitation without any fitted parameters we were

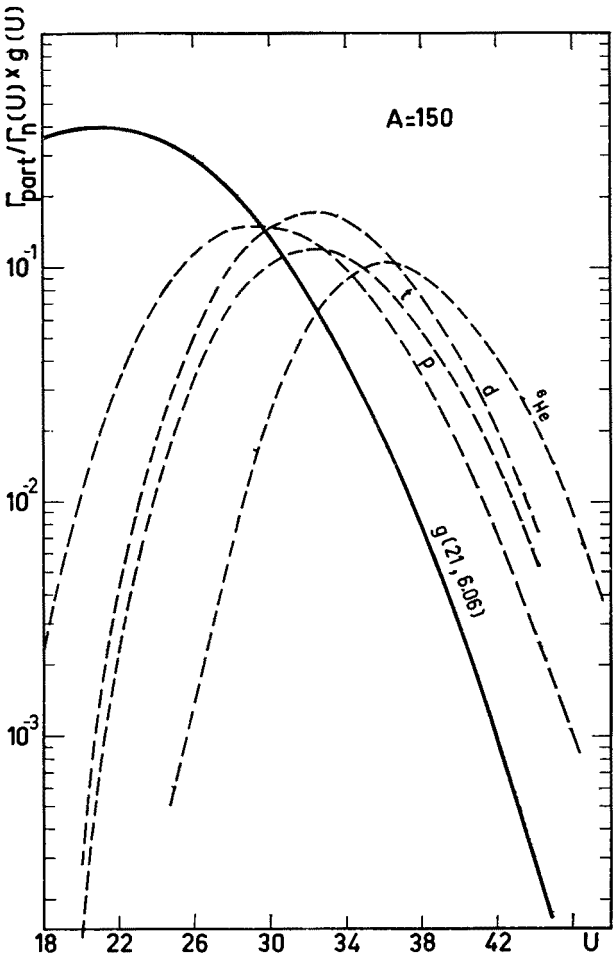

Fig. 29. Excitation energy distribution of fragments emitting the charged particles. The results concern the evaporation from the $A = 150$ nucleus (intensities are not to scale). The solid line gives the excitation energy distribution of the "normal" (neutron emitting, binary fission) fragments of the same mass

able to reproduce experimental values of the mean fragment masses in the case of emission at an angle $\theta \approx 0°$ (in the case of emission along the heavy fragment trajectory the masses were not determined experimentally). The calculated intensity of emission from the heavy fragment is in agreement with experiment within the uncertainties of the parameters used. The measured α-particle spectra can be also explained in terms of this hypothesis if one takes account the fact of non-sphericity of the *L*-fragments. On the other hand there are severe difficulties in explaining the intensity of emission from the light fragments. The fact that emission from these fragments is more intense than from the heavy ones seems to be established with full confidence, but we are able to explain this only by assuming a very low value of the moment of inertia of the *L*-fragment or the high angular momentum of this nucleus. A strangely low value of J is needed also for explaining the strong anisotropy observed, but the experimental result is in this case less sure. Besides, the theory did not take into account some apparently important factors.

One can say that it is owing this puzzling difficulties that the problem is interesting at all, but we should like to note that irrespective of them this phenomenon can be exploited as a source of information on the fission fragments. Moreover, if our hypothesis is true, the measurement of the charged particles in the shadow of the fragments is unique in two aspects: the in-flight emission makes easier the measurement of the evaporation spectra in the full energy range and, what is even more important, it may appear to be a rare case of charged particle evaporation from the highly excited nuclei not contamined by a direct reaction, which usually hinders the statistical model testing.

We wish to express our gratitude to Professor Z. Sujkowski for his continuous interest in this work. Thanks are due to Drs A. Dudek and Z. Majka for information on the optical model parameters.

REFERENCES

[1] E. Piasecki, M. Dakowski, T. Krogulski, J. Tys, J. Chwaszczewska, *Phys. Lett.*, **33B**, 568 (1970).
[2] E. Piasecki, J. Błocki, *Nucl. Phys.*, **A208**, 381 (1973).
[3] I. Halpern, *Ann. Rev. Nucl. Sci.*, **21**, 245 (1971).
[4] M. Asghar, R. Chastel, T. P. Doan, *Report* PNB 120 (1971).
[5] T. Ericson, *Adv. Phys.*, **9**, 425 (1960).
[6] K. Skarsvag, K. Bergheim, *Nucl. Phys.*, **45**, 72 (1963).
[7] H. R. Bowman, S. G. Thompson, J. C. D. Milton, W. J. Świątecki, *Phys. Rev.*, **126**, 2120 (1962); **129**, 2133 (1963).
[8] C. P. Sargent, W. Bertozzi, P. T. Demos, J. L. Matthews, W. Turchinetz, *Phys. Rev.*, **137**, B89 (1965).
[9] Gy. Kluge, *Report* KFKJ-71-55.
[10] M. V. Blinov, N. M. Kazarinov, I. T. Krisuk, A. N. Protopopov, *Yad. Fiz.*, **12**, 41 (1970).
[11] T. D. Thomas, *Nucl. Phys.*, **53**, 552 (1964).
[12] J. R. Grover, J. Gilat, *Phys. Rev.*, **157**, 802 (1967).
[13] D. G. Sarantites, B. D. Pate, *Nucl. Phys.*, **A93**, 545; 567 (1967).
[14] A. Gilbert, A. G. W. Cameron, *Can. J. Phys.*, **43**, 1446 (1965).
[15] D. Sperber, *Report* NYO-2961 (1961).

[16] G. T. Garvey, W. J. Gerace, R. L. Jaffe, I. Talmi, I. Kelson, *Rev. Mod. Phys.*, **41**, No 4 — Supplement (1969).
[17] H. W. Schmitt, J. H. Neiler, F. J. Walter, *Phys. Rev.*, **141**, 1146 (1966).
[18] A. C. Wahl, A. E. Norris, R. A. Rouse, J. C. Williams, *Physics and Chemistry of Fission*, Vienna 1969, p. 813.
[19] M. R. Iyer, A. K. Ganguly, *Phys. Rev.*, **C3**, 785 (1971).
[20] P. Armbruster, *Nucl. Phys.*, **A140**, 385 (1970).
[21] E. Konecny, H. Gunther, H. Rösler, G. Siegert, H. Ewald, *Z. Phys.*, **231**, 59 (1970).
[22] W. Reisdorf, J. P. Unik, H. C. Griffin, L. E. Glendenin, *Nucl. Phys.*, **A177**, 337 (1971).
[23] G. I. Marchuk, V. E. Kolesov, *Primienenye chislennykh metodov dla raschota neutronnykh sechenii*, Atomizdat, Moskva 1970.
[24] A. Dudek, *Report* INP 689/PL (1969).
[25] J. R. Huizenga, G. Igo, *Nucl. Phys.*, **29**, 462 (1962).
[26] J. H. Carver, G. E. Coote, T. R. Sherwood, *Nucl. Phys.*, **37**, 449 (1962).
[27] H. K. Vonach, J. R. Huizenga, *Phys. Rev.*, **149**, 844 (1966).
[28] S. G. Nilsson, O. Prior, *Mat. Fys. Medd. Dan. Vid. Selsk.*, **32**, No 16 (1960).
[29] K. Pomorski, *Thesis*, Report INR, 1412/VII/PL (1972).
[30] N. D. Dudey, T. T. Sugihara, *Phys. Rev.*, **139**, B896 (1965).
[31] H. K. Vonach, R. Vandenbosch, J. R. Huizenga, *Nucl. Phys.*, **60**, 70 (1964).
[32] D. G. Sarantites, E. J. Hoffman, *Nucl. Phys.*, **A180**, 177 (1972).
[33] R. A. Esterlund, B. D. Pate, *Nucl. Phys.*, **69**, 401 (1965).
[34] T. D. Thomas, *Ann. Rev. Nucl. Sci.*, **18**, 406 (1968).
[35] O. Nathan, S. G. Nilsson, $\alpha-\beta-\gamma$ *Spectroscopy*, North Holland Publishing Company (1965) p. 601.
[36] J. R. Nix, W. J. Świątecki, *Nucl. Phys.*, **71**, 1 (1965); J. R. Nix, *Nucl. Phys.*, **130**, 241 (1969).
[37] B. I. Medvedev, *Yad. Fiz.*, **13**, 17 (1971).
[38] E. Erba, U. Facchini, E. Saetta-Menichella, *Nuovo Cimento*, **22**, 1237 (1961).
[39] U. Facchini, E. Saetta-Menichella, *Energia Nucleare*, **15**, 54 (1968).
[40] M. T. Magda, A. Alevra, I. R. Lukas, D. Plostinaru, E. Trutia, M. Molea, *Nucl. Phys.*, **A140**, 23 (1970).
[41] U. Facchini, E. Saetta-Menichella, *Acta Phys. Pol.*, **A38**, 537 (1970).
[42] K. S. Thind, R. H. Tomlinson, *Can. J. Phys.*, **48**, 3016 (1970).
[43] A. R. de L. Musgrove, *Report* AAEC/E211 (1970).
[44] A. R. de L. Musgrove, private communication.
[45] T. D. Newton, *Can. J. Phys.*, **34**, 804 (1956).
[46] P. F. A. Klinkenberg, *Rev. Mod. Phys.*, **24**, 63 (1952).
[47] N. N. Abdelmalek, V. S. Stavinsky, *Nucl. Phys.*, **58**, 601 (1964).
[48] D. W. Lang, *Nucl. Phys.*, **26**, 434 (1961).
[49] J. N. Schubin, A. V. Malyshev, V. S. Stavinsky, *Conference on Nuclear Data*, CN-23/106, Paris 1969.
[50] D. W. Lang, *Nucl. Phys.*, **53**, 113 (1964).
[51] D. Bodansky, *Ann. Rev. Nucl. Sci.*, **12**, 122 (1962).
[52] J. Benveniste, G. Merkel, A. Mitchell, *Phys. Rev.*, **C2**, 500 (1970).
[53] G. E. Gordon, N. K. Aras, *Symposium on Phys. and Chem. of Fission*, Salzburg 1965, vol. II, p. 73.
[54] J. M. Ferguson, P. A. Read, *Phys. Rev.*, **139B**, 56 (1965); **150**, 1018 (1966).
[55] V. P. Zommer, A. E. Saveliev, A. I. Prokofiev, *At. Ener.*, **19**, 116 (1965).
[56] K. S. Thind, B. L. Tracy, H. G. Thode, R. H. Tomlinson, *Physics and Chemistry of Fission*, Vienna 1969, p. 845.
[57] M. V. Blinov, N. M. Kazarinov, I. T. Krisuk, S. S. Kovalenko, *Yad. Fiz.*, **10**, 923 (1969).
[58] A. Gavron, Z. Fraenkel, *Phys. Rev. Lett.*, **27**, 1148 (1971).
[59] L. G. Moretto, *Nucl. Phys.*, **A182**, 641 (1972).

[60] T. D. Thomas, J. R. Grover, *Phys. Rev.*, **159**, 980 (1967).
[61] H. Nifenecker, *These*, Orsay, Report No 4121 (1970).
[62] C. Signarbieux, J. Poitou, M. Ribrag, J. Matuszek, *Phys. Lett.*, **39B**, 503 (1972).
[63] M. R. Iyer, A. K. Ganguly, *Phys. Rev.*, **C5**, 1410 (1972).
[64] V. M. Strutinsky, *Sov. Phys. JETP*, **37**, 861 (1959).
[65] I. F. Croall, H. J. Willis, *J. Inorg. Nucl. Chem.*, **25**, 1213 (1963).
[66] D. G. Sarantites, G. E. Gordon, C. D. Coryell, *Phys. Rev.*, **138B**, 353 (1965).
[67] H. Warhanek, R. Vandenbosch, *J. Inorg. Nucl. Chem.*, **26**, 669 (1964).
[68] S. S. Kapoor, R. Ramanna, *Phys. Rev.*, **133B**, 598 (1964).
[69] M. M. Hoffman, *Phys. Rev.*, **133B**, 714 (1964).
[70] H. Labus, *Report* Jül-643-FN (1970).
[71] J. B. Wilhelmy, E. Cheifetz, R. C. Jared, S. G. Thompson, H. R. Bowman, J. O. Rasmussen, *Report* UCRL-20426, 161 (1971).
[72] J. O. Rasmussen, W. Nörenberg, H. J. Mang, *Nucl. Phys.*, **A136**, 465 (1969).
[73] J. M. Blatt, V. F. Weisskopf, *Theoretical Nuclear Physics*, J. Wiley and Sons, N. York 1952, p. 367.
[74] D. C. Williams, T. D. Thomas, *Nucl. Phys.*, **A92**, 1 (1967).
[75] I. Ragnarsson, *Proceedings Conf. Leysin*, CERN 1970, 70–30, p. 847.
[76] W. D. Myers, W. J. Świątecki, *Report* UCRL-11980 (1965).
[77] E. Cheifetz, R. C. Jared, S. G. Thompson, J. B. Wilhemy, *Phys. Rev. Lett.*, **25**, 38 (1970).
[78] J. K. Poggenburg, H. J. Mang, J. O. Rasmussen, *Phys. Rev.*, **181**, 1697 (1969).
[79] M. L. Choudhury, *J. Phys.*, **A4**, 328 (1971).
[80] W. J. Świątecki, *Second Conf. on the Peaceful Uses of Atomic Energy*, Geneva 1958, vol. 15, p. 248.
[81] A. C. Douglas, N. MacDonald, *Nucl. Phys.*, **13**, 382 (1959).
[82] G. Liggett, D. Sperber, *Phys. Rev.*, **C3**, 167 (1971).
[83] H. K. Vonach, J. R. Huizenga, *Phys. Rev.*, **149**, 844 (1966).
[84] Y. Kanda, *Nucl. Phys.*, **A185**, 177 (1972).
[85] J. Benveniste, G. Merkel, A. Mitchell, *Phys. Rev.*, **141**, 980 (1966); **174**, 1357 (1968).
[86] M. Bormann, H. H. Bissem, E. Magiera, R. Warnemunde, *Nucl. Phys.*, **A157**, 481 (1970).
[87] I. Kumabe, *J. Phys. Soc. Jap.*, **13**, 325 (1958).
[88] L. I. Prokhorova, R. E. Bagdasarov, I. I. Kostukhov, V. G. Nesterov, B. Nurpeysov, G. N. Smirenkin, J. M. Turchin, *At. Energ.*, **30**, 250 (1971).
[89] M. Rajagopalan, T. D. Thomas, *Phys. Rev.*, **C5**, 1402 (1972).
[90] F. G. Perey, *Phys. Rev.*, **131**, 745 (1963).
[91] M. A. Melkanoff, T. Sawada, N. Cindro, *Phys. Lett.*, **2**, 98 (1962).
[92] P. E. Hodgson, *Adv. Phys.*, **17**, 563 (1968).
[93] O. F.Niemiec, A. T. Rudchik, L. S. Sokolov, V. V. Tokarevski, I. P. Chernov, *Izv. Akad. Nauk SSSR, Ser. Fiz.*, **31**, 532 (1967).
[94] P. E. Hodgson, *Nuclear Reactions and Nuclear Structure*, Clarendon Press, Oxford 1971.
[95] M. Dakowski, J. Chwaszczewska, T. Krogulski, E. Piasecki. M. Sowiński, *Phys. Lett.*, **25B**, 213 (1967).